ADVANCED THERAPEUTICS
www.advtherap.com

Id1 and Id3 Are Regulated Through Matrix-Assisted Autocrine BMP Signaling and Represent Therapeutic Targets in Melanoma

*Georg Sedlmeier, Vanessa Al-Rawi, Justyna Buchert, Klaus Yserentant, Melanie Rothley, Anastasia Steshina, Simone Gräßle, Ruo-Lin Wu, Thomas Hurrle, Wilfrid Richer, Charles Decraene, Wilko Thiele, Jochen Utikal, Wasim Abuillan, Motomu Tanaka, Dirk-Peter Herten, Caroline S. Hill, Boyan K. Garvalov, Nicole Jung, Stefan Bräse, and Jonathan P. Sleeman**

The tumorigenicity of cancer cells is highly influenced by the extracellular matrix (ECM) through mechanisms that are poorly understood. Here it is reported that a variety of 3D ECM microenvironments strongly induce expression of Id1 and Id3 in melanoma cells. Genetic ablation of Id1/Id3 impairs melanoma cell outgrowth in 3D Matrigel culture and inhibits melanoma initiation in vivo. Mechanistically, 3D ECM microenvironments hinder diffusion of endogenously produced bone morphogenetic proteins, thereby fostering autocrine signaling and Id1/Id3 expression. A compound screen identifies new coumarin derivatives that potently inhibit both Id1/Id3 expression and melanoma initiation in vivo. Together, the findings reveal a novel mechanism through which the ECM increases tumorigenicity, identify Id1/Id3 as melanoma-relevant therapeutic targets, and characterize inhibitors of Id1/Id3 expression with therapeutic potential.

1. Introduction

Phenotypic plasticity is thought to enable a subpopulation of tumor cells to support the initiation, long-term maintenance and therapy resistance of tumors.[1] Plasticity can be acquired by tumor cells through exposure to appropriate environmental signals.[2] The extracellular matrix (ECM) within the tumor microenvironment, a complex and dynamic network of secreted proteins and polysaccharides that includes collagens, laminins, proteoglycans and hyaluronic acid,[3] is thought to provide such signals through its biochemical and physical properties.[4–6] In mice, the efficiency of tumor initiation increases with the

Dr. G. Sedlmeier, Dr. V. Al-Rawi, Dr. J. Buchert, Dr. M. Rothley, A. Steshina, Dr. R.-L. Wu, Dr. W. Thiele, Dr. B. K. Garvalov, Prof. J. P. Sleeman
European Center for Angioscience (ECAS)
Medical Faculty Mannheim of the University of Heidelberg
Ludolf-Krehl-Strasse 13–17, 68167 Mannheim, Germany
E-mail: jonathan.sleeman@medma.uni-heidelberg.de

Dr. G. Sedlmeier, Dr. W. Thiele, Dr. B. K. Garvalov, Prof. J. P. Sleeman
Mannheim Institute for Innate Immunoscience (MI3)
Medical Faculty Mannheim of the University of Heidelberg
Ludolf-Krehl-Strasse 13–17, 68167 Mannheim, Germany

Dr. V. Al-Rawi, Dr. M. Rothley, Dr. W. Thiele, Prof. J. P. Sleeman
Institute of Biological and Chemical Systems – Biological Information Processing (IBCS-BIP)
Karlsruhe Institute of Technology
Campus North, Building 319, Hermann-von-Helmholtz-Platz 1, 76344 Eggenstein-Leopoldshafen, Germany

The ORCID identification number(s) for the author(s) of this article can be found under https://doi.org/10.1002/adtp.202000065

DOI: 10.1002/adtp.202000065

K. Yserentant, Dr. W. Abuillan, Prof. M. Tanaka, Prof. D.-P. Herten
Institute of Physical Chemistry
University of Heidelberg
Im Neuenheimer Feld 229, 69120 Heidelberg, Germany

K. Yserentant, Prof. D.-P. Herten
College of Medical and Dental Sciences & School of Chemistry
University of Birmingham
Birmingham, UK

K. Yserentant, Prof. D.-P. Herten
Centre of Membrane Proteins and Receptors (COMPARE)
Universities of Birmingham and Nottingham
UK

S. Gräßle, Dr. T. Hurrle, Dr. N. Jung, Prof. S. Bräse
Institute of Organic Chemistry (IOC)
Karlsruhe Institute of Technology
Campus South, Building 30.42, Fritz-Haber-Weg 6 76131 Karlsruhe, Germany

S. Gräßle, Dr. N. Jung, Prof. S. Bräse
Institute of Biological and Chemical Systems – Functional Molecular Systems (IBCS-FMS)
Karlsruhe Institute of Technology (KIT)
Hermann-von-Helmholtz-Platz 1 D-76344 Eggenstein-Leopoldshafen Germany

severity of immunodeficiency, and through co-injection of tumor cells with Matrigel, a basement membrane-like mixture of ECM components.[7] These observations underscore the critical role that the tumor microenvironment, and in particular the ECM plays in regulating the tumorigenicity of cancer cells.

Malignant melanoma is the most lethal form of skin cancer. Although targeted therapy and immunotherapy are improving patient survival, the management of patients with metastatic disease remains a major challenge in the clinic, for example due to lack of response or the acquisition of resistance mutations during immunotherapy.[8–10] Melanoma cells exhibit a particularly high degree of plasticity that is thought to be due at least in part to their sensitivity to microenvironmental changes.[11–14] Notably, the composition of the extracellular matrix surrounding melanoma cells regulates tumor cell plasticity.[7,15] These observations suggest that targeting ECM-induced tumorigenesis may represent a novel approach to melanoma therapy. However, the mechanisms through which the ECM impacts on the tumorigenicity of melanoma cells remains to be determined.

Inhibitor of DNA binding 1 and 3 (Id1 and Id3) are transcriptional regulators whose expression is regulated by bone morphogenetic protein (BMP) and transforming growth factor β (TGF-β) signaling.[16,17] They act as dominant negative inhibitors of basic helix-loop-helix (bHLH) transcription factors, by heterodimerizing with them and preventing them from binding to DNA.[18] Expression of Id1 and Id3 has been implicated in tumor initiation and metastatic growth.[19–21] Accordingly, their expression correlates with poor prognosis for many types of cancer,[22] including melanoma.[23] Loss of Id3 results in an impaired B-cell proliferation that can be rescued by ectopic overexpression of Id1,[24] indicating functional redundancy between Id1 and Id3.

Dr. W. Richer, Dr. C. Decraene
CNRS UMR144
Translational Research Department
Institut Curie
PSL Research University
26 rue d'Ulm, Paris Cedex 05 75248, France
Prof. J. Utikal
Skin Cancer Unit
German Cancer Research Center (DKFZ)
Im Neuenheimer Feld 280, 69120 Heidelberg, Germany
Prof. J. Utikal
Department of Dermatology, Venereology and Allergology
University Medical Center Mannheim
Ruprecht-Karl University of Heidelberg
Theodor-Kutzer-Ufer 1–3, 68167 Mannheim, Germany
Prof. M. Tanaka
Center for Integrative Medicine and Physics
Institute for Advanced Study
Kyoto University
Yoshida Ushinomiya-cho
Sakyo-Ku
Kyoto 606-8501, Japan
Prof. M. Tanaka
Center for Integrative Medicine and Physics
Institute for Advanced Study, Kyoto University
Kyoto 606-8501 Japan
Dr. C. S. Hill
The Francis Crick Institute
1 Midland Rd London NW1 1AT, UK

Table 1. Co-injection of melanoma cells with ECM components into syngeneic mice enhances tumor initiation. Different numbers of melanoma cells (B16-F10, Ret) were injected into syngeneic mice together with PBS, Matrigel (10 mg mL^{-1}), laminin I (4.5 mg mL^{-1}), collagen I (3.4 mg mL^{-1}) or fibronectin (625 µg mL^{-1}) to calculate the tumor initiating cell (TIC) frequency in vivo. The number of animals with a tumor > 1000 mm^3 in size is indicated for each group. Tumor growth was monitored for 3 months. The tumor initiating cell (TIC) frequency was calculated using extreme limiting dilution analysis (ELDA) software.[59] *p*-values refer to the comparison with the PBS control.

Number of animals with tumors/total number of injected animals								
Cell line	Injection with	Number of injected cells					TIC frequency	*p*-value
		5000	500	100	50	10		
B16-F10	PBS	6/6	1/10	0/4	0/6	N.D.	1/2158	
	Matrigel	6/6	6/6	N.D.	11/11	5/5	1/1	<0.001
	laminin I	N.D.	5/5	6/6	N.D.	4/6	1/9	<0.001
	collagen I	N.D.	N.D.	4/5	N.D.	0/6	1/80	0.055
	fibronectin	N.D.	N.D.	0/6	N.D.	0/6	N.D.	0.441
		Number of injected cells					TIC frequency	*p*-value
		1000	100	10				
Ret	PBS	2/6	0/6	0/6			1/2800	
	Matrigel	5/5	9/10	5/5			1/23	<0.001
	laminin I	6/6	5/6	6/6			1/23	<0.001

Here we report that a variety of 3D ECM environments induce Id1 and Id3 expression in melanoma cells through matrix-assisted autocrine BMP signaling. Genetic ablation of Id1 and Id3 expression suppressed melanoma cell outgrowth and invasiveness in 3D ECM, and inhibited melanoma initiation and growth in vivo. Through synthesizing and screening a custom targeted chemical library, we identified a novel substance class that inhibits Id1 and Id3 expression. In proof of principle experiments, one of the most promising of these compounds was investigated further and found to exert a strong inhibitory effect on ECM-mediated Id1 and Id3 expression, and to potently suppress melanoma initiation and growth in experimental animals. These data suggest that Id1 and Id3 represent promising therapeutic targets for melanoma, and identify a new class of chemical inhibitors of Id1 and Id3 that can serve as lead compounds for drug development.

2. Results

2.1. Multiple ECM Environments Promote Melanoma Initiation In Vivo

Co-injection with Matrigel can profoundly increase the ability of tumor cells to initiate and grow as tumors in mice.[7,25] In severely immunocompromised mice, a single melanoma cell co-injected with Matrigel suffices to initiate a tumor.[7] To investigate whether increased tumor initiation is specific to particular ECM environments, we co-injected B16-F10 melanoma cells together with various ECM components into immunocompetent syngeneic mice. Co-injection with Matrigel and laminin I strongly increased the tumor initiating cell (TIC) frequency (**Table 1**). The TIC frequency

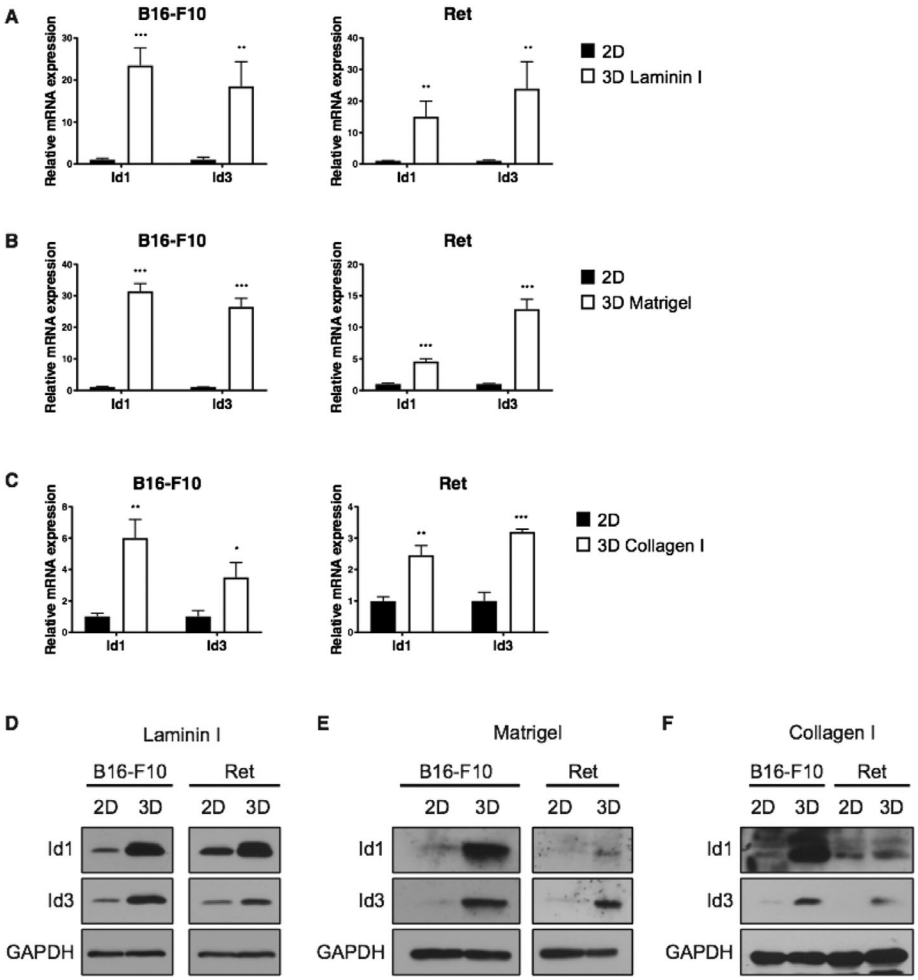

Figure 1. Murine melanoma cells exhibit significantly increased Id1 and Id3 expression in 3D ECM environments. A) B16-F10 (left) or Ret (right) cells were cultured for 72 h in 2D culture or 3D laminin I (4.5 mg mL^{-1}), B) 3D Matrigel (10 mg mL^{-1}) or C) 3D collagen I (4 mg mL^{-1}) culture. Relative Id1 and Id3 mRNA expression were measured via qRT-PCR. Rplp0 served as a housekeeping gene. $n = 3$. Student's t-test: $^{*}p < 0.05$, $^{**}p < 0.01$, $^{***}p < 0.001$. Error bars = SEM. D) Western Blot analysis of Id1 and Id3 protein expression in B16-F10 and Ret cells cultured in 3D laminin I, E) 3D Matrigel (10 mg mL^{-1}) or F) collagen I (4 mg mL^{-1}) for 72 h, compared to cells cultured in 2D.

also showed a trend toward an increase after co-injection with collagen type I, but not with fibronectin (Table 1). Similar experiments with Ret melanoma cells confirmed the robust increase in TIC frequency upon co-injection with Matrigel or laminin I into syngeneic mice (Table 1). Tumor growth was also increased when the melanoma cells were co-injected with these ECM components (Figure S1A, Supporting Information). Thus, increased tumorigenicity of melanoma cells is induced by a number of ECM environments, and is not limited to Matrigel.

2.2. ECM Environments Induce Id1 and Id3 Expression

To identify changes in transcription that underlie the increased TIC frequency in response to a defined 3D laminin I environment, we compared transcriptional profiles between B16-F10 and Ret melanoma cells cultured as a monolayer on standard plastic surfaces (2D), embedded in 3D laminin I (3D Laminin), or embedded in 3D methylcellulose (3D MC) as a control (Figure S1B, Supporting Information). Strikingly, for both melanoma cell lines, the most highly upregulated genes in 3D laminin I culture were Id1, Id3, and Smad6 (Table S1, Supporting Information), archetypal TGF-β and BMP response genes.[16,17] While Smad6 negatively regulates TGF-β and BMP signaling,[26,27] Id1 and Id3 have been implicated in governing the self-renewal properties of stem cells,[28] and in promoting tumor initiation by colon and breast cancer cells.[19–21] In further experiments, we therefore focused on Id1 and Id3 as potential mediators of the pro-tumorigenic properties of 3D ECM environments.

We first confirmed by real-time PCR that Id1 and Id3 mRNA expression is strongly upregulated in B16-F10 and Ret melanoma cells grown in 3D laminin I compared to 2D (**Figure 1**A). Furthermore, Id1 and Id3 expression was significantly upregulated in 3D Matrigel and 3D collagen type I at the mRNA level (Figure 1B,C). Consistently, Id1 and Id3 protein levels were increased in all three 3D ECM environments compared to 2D conditions (Figure 1D–F). Thus upregulation of Id1 and Id3 is a common feature of ECM environments that promote tumor initiation.

To determine whether these observations hold true for other types of cancer, we co-injected 4T1 murine breast cancer cells with Matrigel into syngeneic mice, and found a strong increase in

Table 2. Loss of Id1 and Id3 expression significantly reduces tumor initiation in vivo measured at days 28–30. Five or fifty B16-F10 or Ret control or Id1/Id3 KO cells were co-injected with Matrigel (10 mg mL^{-1}) into syngeneic mice. Each group (control or Id1/Id3 KO) consists of 24 animals (eight animals for each of the three cell clone tested). Tumor initiation was scored when tumors with a size of more than 1000 mm^3 were present 28–30 days after tumor cell injection. The tumor initiating cell (TIC) frequency was calculated using extreme limiting dilution analysis (ELDA) software.[59].

		Number of animals with tumors/total number of injected animals			
Cell line	CRISPR targeting	5 cells injected	50 cells injected	TIC frequency	*p*-value
B16-F10	control	4/24	17/24	1/38	0.0271
	Id1/Id3	1/24	11/24	1/85	
Ret	control	7/24	20/24	1/24	<0.001
	Id1/Id3	1/24	7/24	1/142	

TIC frequency (Table S2, Supporting Information). Furthermore, Id1 and Id3 expression was robustly upregulated in 4T1 cells in response to 3D laminin I, Matrigel and collagen type I culture (Figure S1C–E, Supporting Information). Thus upregulation of Id1 and Id3 in response to 3D ECM environments also occurs in breast cancer cells.

To determine whether exposure to ECM environments results in a durable increase in tumor initiation capacity in vivo, we cultured B16-F10 and Ret cells for 72 h in 3D Matrigel as before, but then removed them from the Matrigel and injected them in PBS into mice. Pre-culturing in Matrigel did not increase tumor initiation in vivo (Table S3, Supporting Information). In other experiments we found that expression of Id1 and Id3 mRNA is reduced to baseline within an hour after removing cells from 3D Matrigel and replating them on 2D culture (Figure S1F, Supporting Information). These results indicate that both enhanced tumor initiation and increased Id1 and Id3 expression require persistent exposure to an inducing 3D ECM environment.

2.3. Id1 and Id3 Promote Tumor Initiation and Growth of Melanoma Cells In Vivo

Upregulation of Id1 and Id3 could conceivably explain why tumor initiation and growth is increased when melanoma cells are co-injected with ECM components in vivo. To investigate this hypothesis, we used CRISPR/Cas9 to successfully abrogate Id1 and Id3 expression in B16-F10 and Ret cells (Figure S2A, Supporting Information). Abrogation of Id1 or Id3, and particularly their simultaneous deletion in Ret cells suppressed tumor growth (Figure S2B, Supporting Information). We therefore continued with double knockout cells to test the effects of Id1 and Id3 on tumor initiation in vivo by B16-F10 and Ret cells. To this end, either 5 or 50 control or Id1/Id3 knockout cells were co-injected with Matrigel into each mouse. While all animals injected with 50 cells eventually developed tumors over a 90-day period, ablation of Id1 and Id3 expression resulted in a significant delay in tumor initiation (**Table 2**). In addition, significantly reduced tumor growth rates in vivo were observed in cells with abrogated Id1 and Id3 (**Figure 2**A and Figure S2C, Supporting Information). Thus Id1 and Id3 are functionally required for tumor initiation and growth by B16-F10 and Ret cells when co-injected with Matrigel in vivo.

Loss of Id1 and Id3 resulted in a significantly impaired colony outgrowth in 3D Matrigel for both B16-F10 and Ret cells (Figure 2B). Furthermore, Ret cells with abrogated Id1/Id3 expression exhibited a significantly less invasive phenotype (Figure 2B). Importantly, there was no significant reduction in the proliferation rate of control and Id1/Id3 KO cells in 2D conditions (Figure S2D, Supporting Information). These data support the notion that elevated Id1 and Id3 expression is critical for efficient cell growth in 3D ECM environments such as Matrigel, which is reflected in the reduced tumor initiation and growth of the Id1/Id3 KO cells co-injected with Matrigel.

2.4. BMP Signaling Induces Id1 and Id3 Expression in 3D ECM

Next, we sought to elucidate why Id1 and Id3 expression is increased in certain 3D ECM environments. As Id1 and Id3 are induced by BMP and TGF-β signaling,[16,17] we inhibited these pathways. Western blot analysis revealed that cells in 3D Matrigel exhibit increased phospho-Smad1 levels, indicative of activation of canonical BMP signaling, which was abrogated by treatment with the BMP type I receptor inhibitor LDN-193189 (LDN)[29] or with recombinant noggin, a naturally occurring BMP antagonist,[30] but not with the TGF-β receptor inhibitor SB-431542 (SB; **Figure 3**A).[31] Importantly, LDN and noggin treatment of B16 and Ret cells completely blocked the induction of both Id1 and Id3 in 3D Matrigel, while SB had no or a less pronounced effect on the levels of the two proteins (Figure 3A). Similarly, BMP signaling was also required for increased Id1 and Id3 expression in 3D laminin and 3D collagen environments (Figure S3A,B, Supporting Information). These data establish BMP signaling as being responsible for increased Id1 and Id3 expression in 3D ECM environments.

2.5. Matrix-Assisted Autocrine BMP Signaling Regulates Id1 and Id3 Expression in 3D ECM

In 3D ECM, BMPs that activate BMP signaling and induce Id1 and Id3 expression could in principle be derived from the culture medium, from the ECM preparations, or from the melanoma cells themselves. The levels of Id1 and Id3 in 3D culture were the same in standard Matrigel prepared with 10% fetal calf serum (FCS), Matrigel with 1% FCS or growth factor-reduced (GFR) Matrigel (Figure S3C, Supporting Information). These results suggest that BMPs derived from the culture medium or contained within the ECM are not responsible for the induction of Id1 and Id3 expression in 3D Matrigel.

Several ECM proteins have the potential to positively regulate BMP signaling through interacting with cell surface receptors.[32] We therefore set out to test whether cell-ECM interactions in 3D culture directly promote BMP signaling, and thereby increase Id1 and Id3 expression. To this end, we used alginate, which lacks epitopes to which cell surface receptors can bind[33] and is free of growth factors. 3D alginate culture strongly induced Id1 and Id3 expression compared to 2D conditions (Figure 3C). Blocking BMP signaling also significantly inhibited the induction of Id1 and Id3 expression in 3D alginate (Figure 3C).

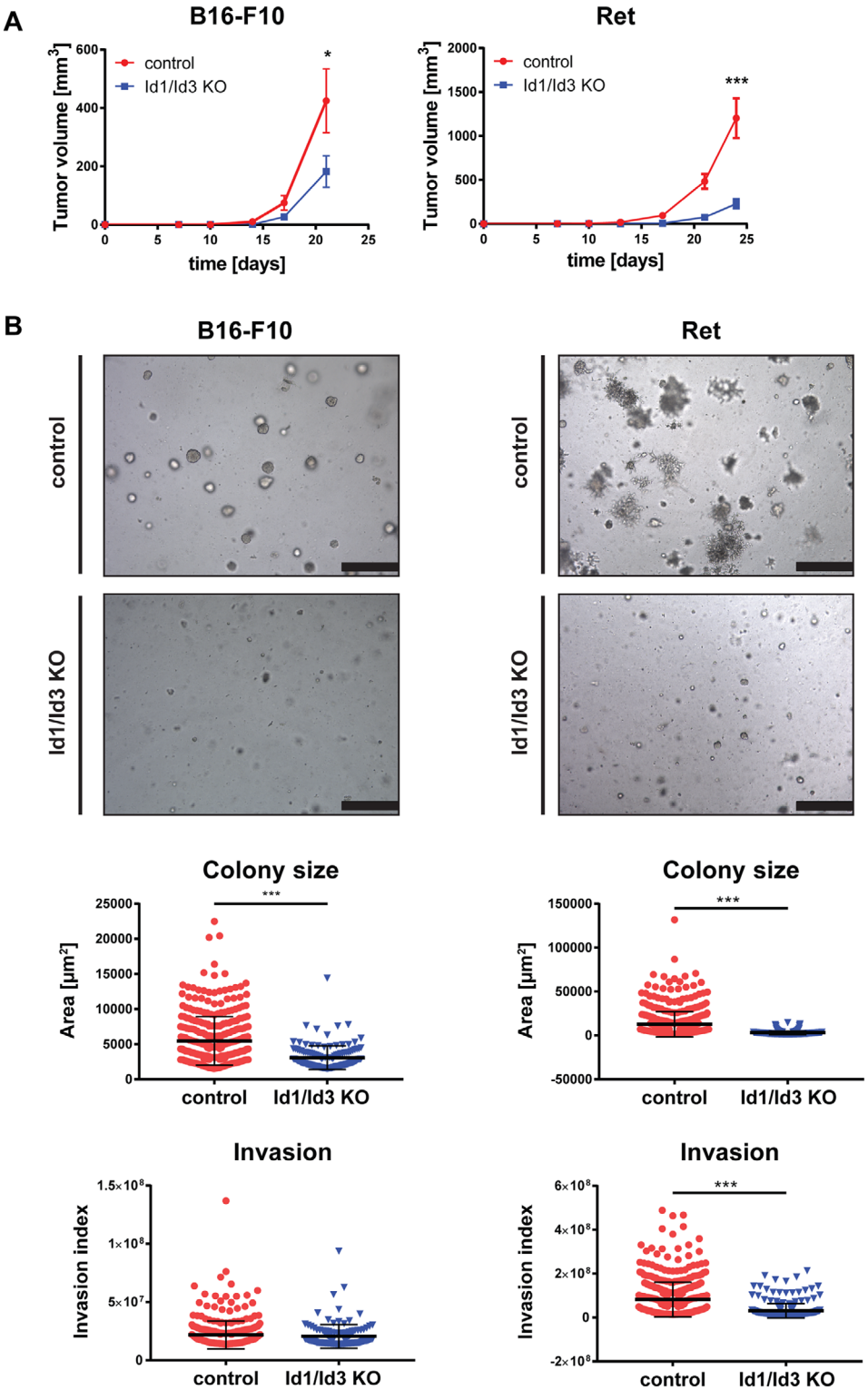

Figure 2. Id1 and Id3 promote melanoma growth. A) Simultaneous Id1 and Id3 gene ablation by CRISPR/Cas9 significantly impairs tumor growth of melanoma cells in vivo. Fifty control or Id1/Id3 KO cells were co-injected with Matrigel (10 mg mL^{-1}) into syngeneic mice. Each group (24 animals per group) consisted of three subgroups of 8 animals each, into which each of the individual clones was transplanted. Nested ANOVA: $*p < 0.05$; $***p < 0.001$. Error bars = SEM. B) Loss of Id1/Id3 expression inhibits the outgrowth and invasion of melanoma cells in 3D Matrigel. B16-F10 or Ret control or Id1/Id3 KO cells were seeded in 3D Matrigel (10 mg mL^{-1}) and incubated for 6 days. Images show control (upper row) and CRISPR/Cas9 cells (lower row) in the 3D culture. Scale bars = 500 µm. Quantification of colony size and invasion index was performed using Fiji image analysis software.[82] Mann–Whitney test: $***p < 0.001$. Error bars = SD.

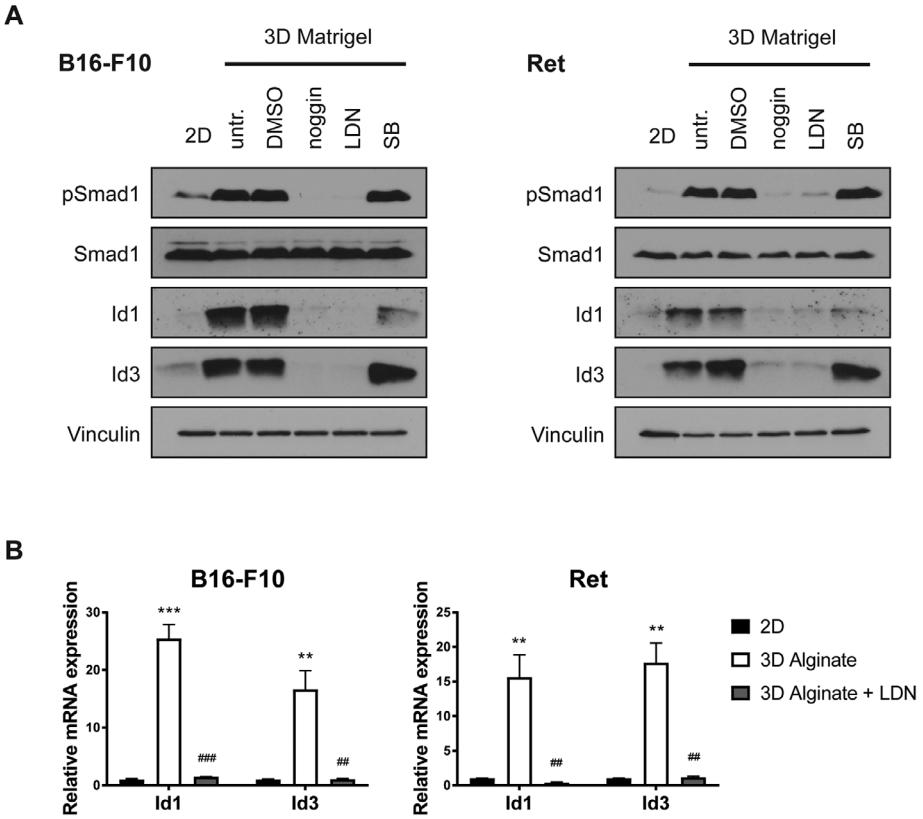

Figure 3. BMP signaling regulates Id1 and Id3 expression in 3D ECM environments. A) Canonical BMP signaling regulates Id1 and Id3 expression. B16-F10 or Ret cells were incubated in 3D Matrigel or standard 2D conditions. Cells cultured in 3D Matrigel were treated at the start of the culture with a single dose of recombinant noggin (300 ng mL^{-1}), LDN-193189 (0.5×10^{-6} M) or SB-431542 (10×10^{-6} M). Id1, Id3, Smad1, phoshpo-Smad1 and Vinculin levels were evaluated by Western blotting. B) Increased Id1 and Id3 expression in murine melanoma cells in 3D alginate. B16-F10 or Ret cells were cultured for 72 h in 0.75% alginate. To block BMP signaling, cells were incubated with LDN-193189 (0.5×10^{-6} M). Id1 and Id3 mRNA expression was compared to 2D cultured cells. $n = 3$. * compared to 2D; # compared to 3D. One-way ANOVA with Tukey's multiple comparisons test: **/##$p < 0.01$, ***/###$p < 0.001$ Error bars = SEM.

The results presented above indicate that neither exogenous growth factors nor cell-matrix interactions are required for upregulated Id1 and Id3 expression in 3D microenvironments, suggesting that melanoma cells themselves may be the source of BMPs that upregulate Id1 and Id3 in 3D ECM. Noggin, which blocks ECM-induced Id1 and Id3 expression (Figure 3A), is an antagonist of BMP2, BMP4, and BMP7,[30] suggesting that melanoma cell-derived BMP2, BMP4, or BMP7 might be responsible for the increased Id1 and Id3 expression in 3D ECM environments. B16-F10 and Ret cells both express BMP4 and BMP7 but not BMP2 at the mRNA level (**Figure 4**A). Transcripts for other BMP ligands could not be detected (data not shown; list of primers in Table S5, Supporting Information). BMP4 and BMP7 proteins were both found in conditioned medium from B16-F10 and Ret cells cultured in 2D conditions (Figure 4B). The sensitivity of available ELISA assays was too low to quantify BMP4 in the conditioned medium. Quantification of BMP7 in the conditioned medium showed that both cell lines secrete low levels of BMP7 (B16-F10: 14.25 pg mL^{-1}; Ret: 3.9 pg mL^{-1}) (Figure 4C). These concentrations are insufficient to induce autocrine expression of Id1 and Id3 under 2D culture conditions, as around 10 ng mL^{-1} of BMP4 and/or BMP7 are required for induction of Id1 and Id3 expression (Figure 4D,E). ECM does not induce BMP4 or BMP7 expression, as no increased expression was observed in cells cultivated in 3D laminin compared to 2D culture (Figure S3D, Supporting Information). Furthermore, we also did not detect consistent upregulation of BMP receptors in 3D Matrigel compared to 2D that could explain increased BMP signaling in 3D conditions (Figure S3E, Supporting Information). In summary, we conclude that B16-F10 and Ret cells secrete low levels of BMP4 and BMP7 that are insufficient to induce autocrine Id1 and Id3 expression under 2D culture conditions.

We reasoned that 3D ECM may have an impact on the diffusion of BMPs, leading to an increased pericellular accumulation of BMPs secreted by cells within the ECM. The resulting locally increased BMP concentrations at the cell surface may thereby become sufficient to induce autocrine BMP-mediated Id1 and Id3 expression. To test this hypothesis, we measured the diffusion coefficient of fluorescently labeled BMP2 in medium, Matrigel or laminin using fluorescence correlation spectroscopy (FCS). The data for BMP2 in medium could be fitted using a simple model for free 3D diffusion of a single fast diffusing species. For both laminin and Matrigel, an additional slowly diffusing species was needed in the fitting to account for the data obtained (Figure S4A–D, Supporting Information). For the fast diffusing species of BMP2 in laminin and Matrigel, similar diffusion coefficients

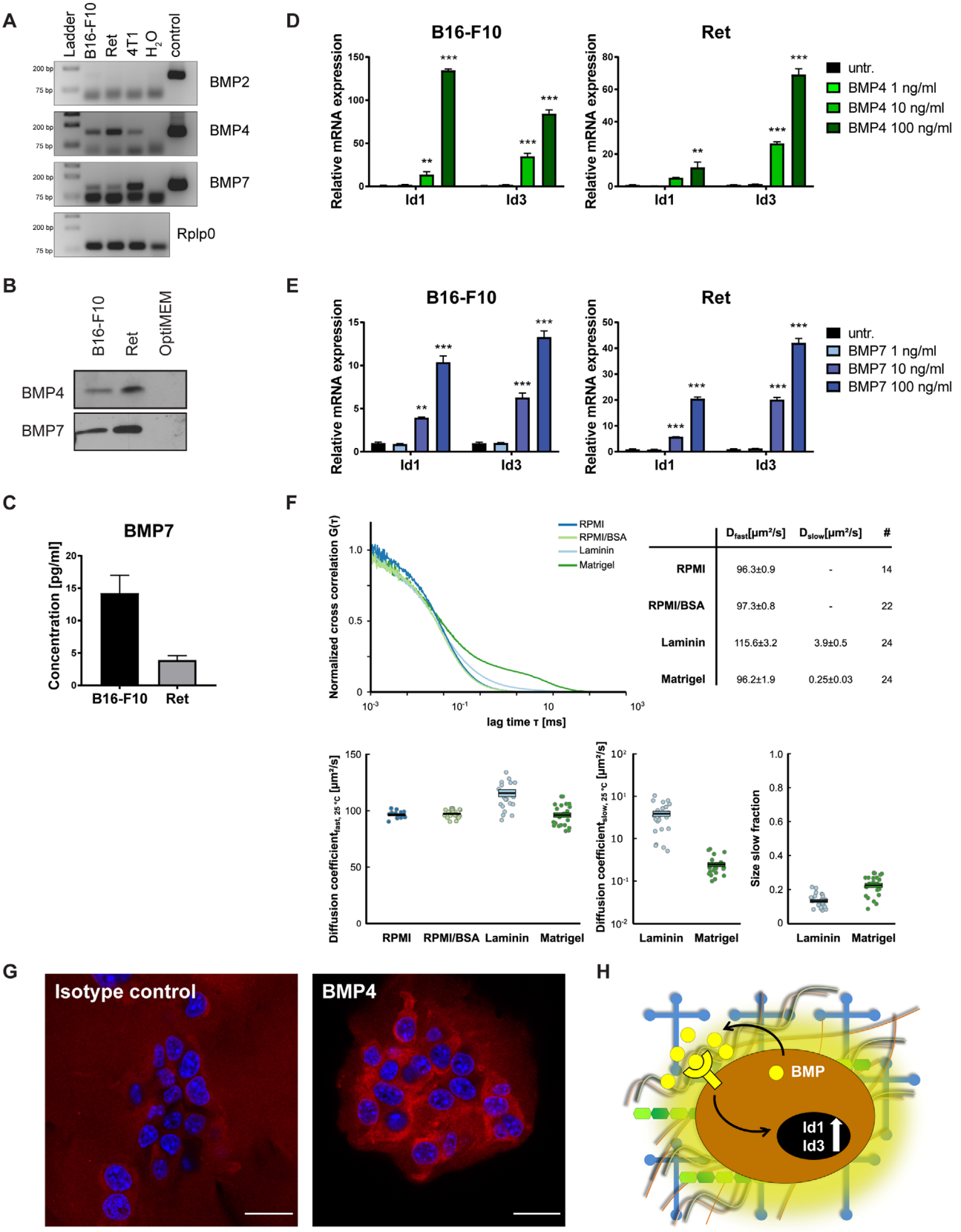

to bulk medium were obtained (Figure 4F). The slowly diffusing species, which is indicative of transient interactions between BMP2 and the 3D ECM gels tested, showed diffusion coefficients of 3.9 ± 0.5 and 0.25 ± 0.03 $\mu m^2 s^{-1}$ for laminin and Matrigel, respectively (Figure 4F). The fraction of slowly diffusing BMP2 was similar for both gels. By contrast, medium supplemented with bovine serum albumin (BSA) at a protein concentration equal to that in 3D Matrigel did not significantly influence the diffusion of BMP2. Therefore, both Matrigel and laminin strongly reduced the diffusion coefficient of BMP2 in the case of the slow species by around 385-fold and 24-fold, respectively, compared to bulk medium (Figure 4F). These data are consistent with the notion that ECM environments can act as barriers that inhibit the diffusion of secreted BMP ligands.

Reduced diffusion would predict that BMP accumulates around cells in 3D Matrigel. To visualize such an accumulation, we performed an immunofluorescence staining for BMP4 in 3D Matrigel-embedded melanoma cells. Consistent with the strongly reduced diffusion of BMP in 3D ECM measured by FCS, we observed a strong pericellular accumulation of BMP4 (Figure 4G). Together, these data are consistent with the notion that endogenously produced BMP4 accumulates around cells grown in 3D ECM due to decreased diffusion. This leads to increased pericellular BMP concentrations that stimulate Id1 and Id3 expression, a mechanism we have termed matrix-assisted autocrine signaling (Figure 4H).

2.6. Correlation of ID1/ID3 Expression with ECM Genes and Invasive Properties in Human Melanoma

To gain insight into the relevance of our findings in murine melanoma cells to human melanoma samples, we first analyzed the skin melanoma cohort of The Cancer Genome Atlas (TCGA). We observed that the expression levels of ID1 and ID3 were very strongly correlated in human melanomas and that the majority of the tumors (54.7%) expressed higher levels of ID1 and/or ID3 than normal skin (**Figure 5**A). We next compiled a list of genes coding for structural ECM components (Table S4, Supporting Information) and tested whether the levels of these genes correlated with those of ID1 and ID3. Intriguingly, the large majority of ECM genes showed a positive correlation with ID1 and ID3 levels, to a significantly higher extent that a random set containing an equal number of genes (Figure 5B). These findings indicate that increased ECM abundance is associated with upregulation of ID1/ID3 expression in human melanomas, similarly to the murine system. To further assess the possible involvement of ID1 and ID3 in human melanoma progression, we analyzed the expression of both genes in a set of human melanoma cell lines from the Heuristic Online Phenotype Prediction (HOPP) database, which uses gene expression signatures to classify melanoma cell lines as proliferative or invasive.[34] The expression of both ID1 and ID3 was significantly higher in invasive melanoma cells, which have been associated with an increased metastatic potential[35] and greater resistance to RAF/MEK inhibitors,[36] the standard of care for a large fraction of melanoma patients. Consistent with other published findings,[23] these data suggest that ID1 and ID3 expression in human melanoma is linked to disease progression and therapy resistance.

2.7. A Targeted Compound Screen Identifies Novel Id1/Id3 Inhibitors

Genetic ablation of Id1 and Id3 expression had a potent inhibitory effect on tumor initiation and growth in vivo, which, together with the data in human melanomas, suggests that these proteins are possible therapeutic targets. We therefore set out to identify novel inhibitors that target Id1 and Id3. As cannabidiol (CBD), a nonpsychotic cannabinoid, has been reported to partially inhibit Id1 expression,[37] we synthesized a unique library containing 62 novel coumarin derivatives that are loosely structurally related to CBD (Data S1, Supporting Information). This library was then screened for compounds that inhibit Id1 and Id3 expression, using CBD as a reference substance. To this end, B16-F10 and Ret melanoma cells were treated with BMP4 (to induce Id1 and Id3 expression) together with each of the compounds individually. The ability of the compounds to inhibit Id1 and Id3 protein expression relative to CBD was assessed using Western blotting

Figure 4. Matrix-assisted autocrine BMP signaling. A) Melanoma cells express BMP4 and BMP7. mRNA expression of BMP2, BMP4 and BMP7 was analyzed in B16-F10 and Ret cells, as well as the murine breast cancer cell line 4T1, by standard PCR of cDNA on a 3% agarose gel. Positive controls were derived from B16-F10 cells transfected with expression plasmids for BMP2, BMP4 and BMP7. Predicted amplicon sizes: BMP2: 154 bp, BMP4: 142 bp, BMP7: 122 bp. B) B16-F10 and Ret cells secrete BMP4 and BMP7. Western blot analysis of conditioned medium detects BMP4 and BMP7 after 48 h in OptiMEM. An OptiMEM medium control lacks a specific band. C) Melanoma cells secrete low levels of BMP7. Supernatants of B16-F10 and Ret cells in 2D culture were analyzed for BMP7 protein levels by ELISA ($n = 2$). D) B16-F10 or Ret cells were serum-starved overnight and treated with increasing concentrations of recombinant BMP4 (1, 10, and 100 ng mL^{-1}; 120-05ET, Peprotech) for 1 h prior to RNA isolation. Relative Id1 and Id3 mRNA expression was determined by qRT-PCR. $n = 3$. One-way ANOVA with Dunnett's multiple comparisons test: $^{**}p < 0.01$, $^{***}p < 0.001$ compared to untreated cells. Error bars = SEM. E) B16-F10 or Ret cells were serum-starved overnight and treated with increasing concentrations of recombinant BMP7 (1, 10, and 100 ng mL^{-1}; 120-03P, Peprotech) for 1 h prior to RNA isolation. Relative Id1 and Id3 mRNA expression was determined by qRT-PCR. $n = 3$. One-way ANOVA with Dunnett's multiple comparisons test: $^{**}p < 0.01$, $^{***}p < 0.001$ compared to untreated cells. Error bars = SEM. F) The diffusion coefficient of BMP2 is strongly reduced in 3D ECM environments. Upper left: Normalized averaged cross-correlation functions for BMP2 diffusion in different environments. Upper right: Table showing the results from fitting the obtained correlation functions (left) with a one- or two-component model for unhindered 3D diffusion. The mean±SEM and the number of measurements per condition (#) is indicated. Lower row: Distribution of individual parameters obtained from fits under the respective conditions. Black horizontal lines indicate means, boxed regions indicates error (SEM). A one-component model was sufficient to fit data from measurements in RPMI and RPMI supplemented with BSA. G) Endogenous BMP4 is concentrated pericellularly in 3D Matrigel. B16-F10 cells were cultured in 3D Matrigel and fixed after 72 h. Cryosections were stained for BMP4 and fluorescence signal detected by a secondary antibody was compared against an isotype antibody control. H) Schematic overview of the mechanism of matrix-assisted BMP signaling in 3D ECM. BMP diffusion is inhibited by ECM components, which leads to increased pericellular concentrations of BMPs that are sufficient to induce autocrine signaling, resulting in the induction of the target genes Id1 and Id3.

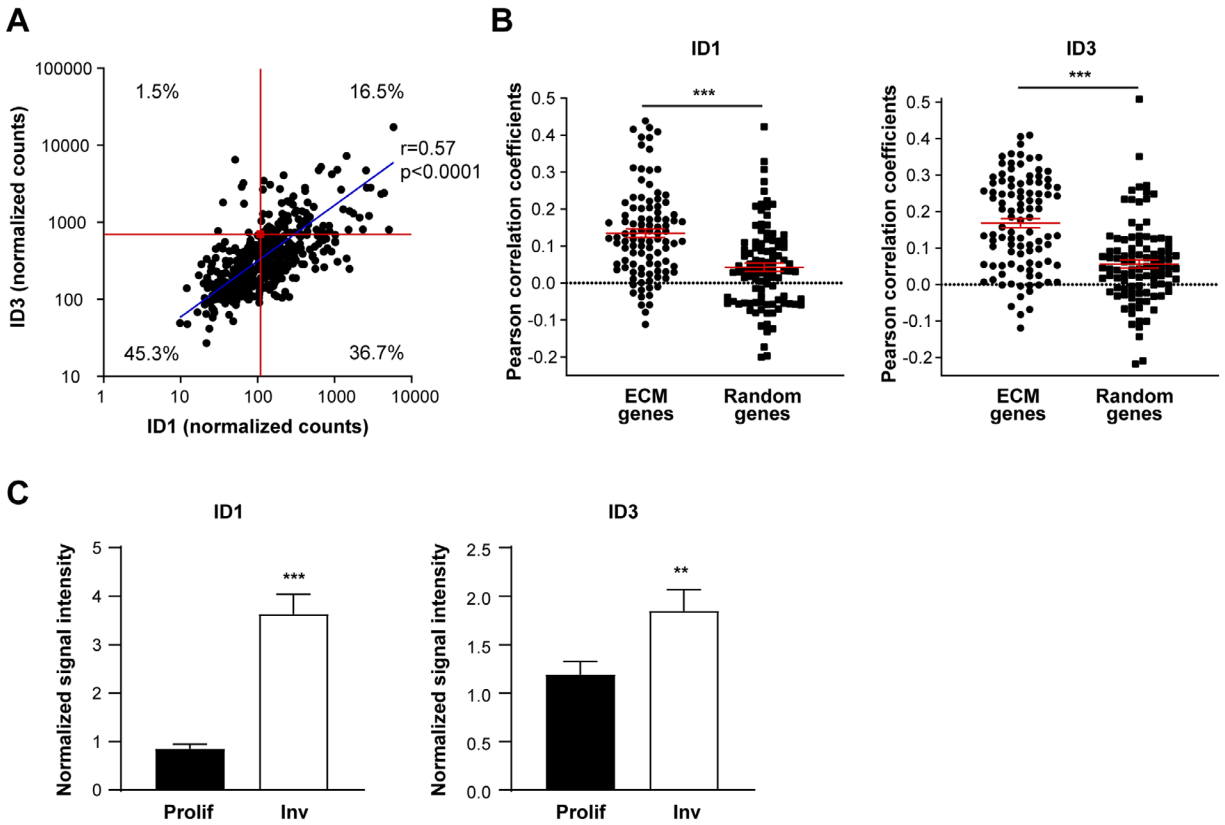

Figure 5. The expression of ID1 and ID3 is linked to increased levels of ECM genes and an invasive phenotype in human melanoma. A) ID1 and ID3 expression is strongly correlated in human melanomas. Expression (normalized RNA-seq reads), of ID1 and ID3 in samples of the cutaneous melanoma cohort of The Cancer Genome Atlas (TCGA). A total of 472 tumor samples were analyzed. The red square indicates expression in normal skin. The percentages indicated on the plot refer to the fractions of tumor samples, which have higher or lower expression of ID1 and/or ID3 than normal skin. *r*, Pearson correlation coefficient. B) The expression of ID1 and ID3 correlates with the expression of ECM genes in human melanoma. The expression of 100 genes coding for structural components of the ECM (Table S4, Supporting Information) was correlated to the expression of ID1 (left panel) and ID3 (right panel) in the TCGA cutaneous melanoma cohort and the Pearson correlation coefficients were plotted. As a control the correlation of ID1 and ID3 with a set of 100 random genes is shown. Student's *t*-test: $***p < 0.001$. Error bars = SEM. C) Increased ID1 and ID3 levels are associated with an invasive phenotype in human melanoma cells. Expression of ID1 and ID3 in human melanoma cell lines with a proliferative and invasive phenotypes, as classified using the Heuristic Online Phenotype Prediction (HOPP) algorithm. Expression was analyzed in 101 proliferative cell lines and 90 invasive cell lines. Student's *t*-test: $**p < 0.01$, $***p < 0.001$. Error bars = SEM.

analysis. Around one third of the compounds had an inhibitory effect on both Id1 and Id3 protein expression (20 out of 62). The screen identified a compound class defined by eight coumarin derivatives that inhibited Id1/Id3 protein expression more potently than CBD (**Figure 6**A,B). Of these compounds, the compound X6632 strongly inhibited BMP4-induced Id1/Id3 expression at a concentration of 10×10^{-6} M (Figure S5A,B, Supporting Information), and potently suppressed 3D ECM-mediated Id1/Id3 expression in cells cultured in 3D Matrigel (Figure 6C).

2.8. The Coumarin Derivative X6632 Strongly Inhibits Melanoma Growth In Vivo

To investigate whether X6632 can inhibit tumor initiation and growth in vivo similarly to genetic ablation of Id1/Id3, B16-F10 or Ret melanoma cells were injected subcutaneously into mice. The mice were treated for the first two weeks following implantation of the melanoma cells with either DMSO as a solvent control, with CBD as a reference compound, or with X6632. Melanoma initiation and growth was then assessed over a period of 90 days. Treatment with CBD led to a slight reduction in tumor growth rates and no improvement in tumor-free survival (Figure 6D,E). By contrast, treatment with X6632 strongly inhibited tumor growth, significantly delayed tumor initiation, and even prevented the formation of any tumors in the majority of mice implanted with B16-F10 cells (Figure 5D,E). Importantly, treatment of mice with X6632 was well tolerated, and no signs of toxicity were observed, whereas CBD-treated mice exhibited treatment-related intestinal injury that became obvious in post-mortem examination. Together, these results demonstrate that X6632 is a novel inhibitor of Id1 and Id3 expression, which shows considerable promise as a lead compound for the development of new anti-cancer therapies.

3. Discussion

Here we report that 3D ECM can induce BMP-dependent up-regulation of Id1 and Id3 in melanoma cells through the novel mechanism of matrix-assisted autocrine signaling. Genetic

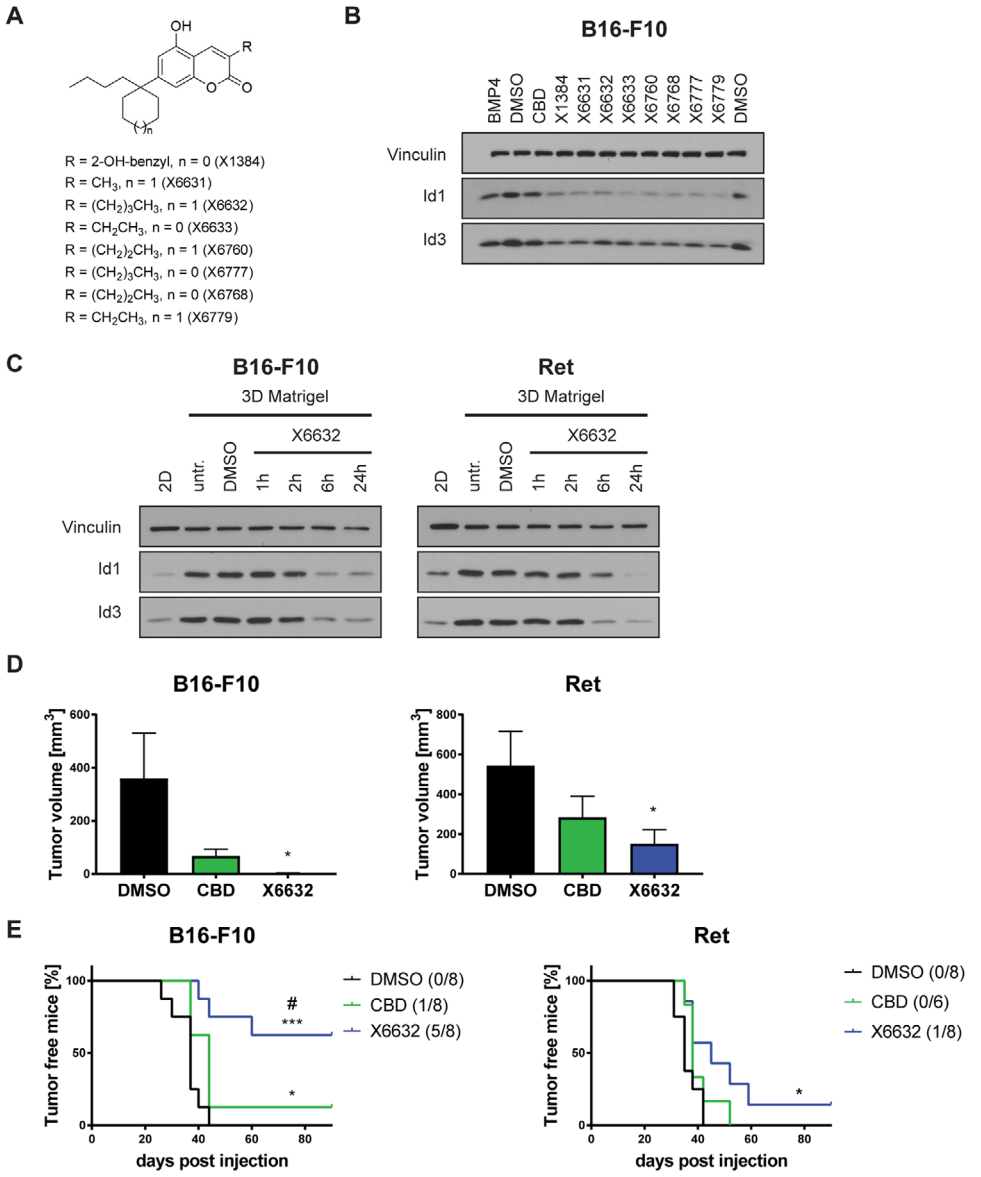

Figure 6. A sub-class of coumarin derivatives exhibits coordinate Id1/Id3 inhibitory activity that is superior to CBD. A) A sub-class of coumarin-type compounds that inhibit Id1 and Id3 expression. B) Eight coumarin compounds of a common sub-class potently inhibit Id1 and Id3 protein expression. B16-F10 and Ret cells were treated with BMP4 (to induce Id1 and Id3 expression) together with the indicated compounds at a concentration of 10×10^{-6} M. DMSO served as a solvent control, CBD served as the reference inhibitor. C) X6632 inhibits 3D ECM-mediated Id1/Id3 expression in melanoma cells cultured in 3D Matrigel. Cells were cultured in 3D Matrigel (5 mg mL^{-1}) for 72 h and treated at the indicated time points with 10×10^{-6} M of X6632 before lysis. D) X6632 significantly inhibits tumor growth in vivo. Fifty B16-F10 or Ret cells were co-injected with Matrigel (10 mg mL^{-1}) into syngeneic mice. Significantly reduced tumor growth was observed in X6632 but not CBD treated mice. Data shows tumor volume at the point when the first animal had to be sacrificed in the DMSO group due to tumors reaching the legal size limit. $n = 6$–8. ANOVA with Fisher's least significant difference test: *$p \leq 0.05$ compared to DMSO. Error bars = SEM. E) X6632 significantly inhibits tumor initiation in vivo. Fifty B16-F10 or Ret cells were co-injected with Matrigel (10 mg mL^{-1}) into syngeneic mice. The percentage of tumor-free mice (tumor volume less than 1000 mm^3) was analyzed over 90 days. $n = 6$–8. * compared to DMSO, # compared to CBD. Log-rank (Mantel-Cox) test: */#$p < 0.05$, ***$p < 0.001$ Error bars = SEM. In panels (D,E) 2 animals injected with Ret cells and treated with CBD died during drug treatment and were excluded from the analyses.

deletion of Id1 and Id3 expression in melanoma cells severely impaired their ability to initiate and sustain tumor growth in experimental animals. In a chemical library screen, we identified a novel substance class that concomitantly inhibits Id1 and Id3 protein expression, which exerted potent anti-cancer activity, while exhibiting no obvious toxicity. These data provide a proof of principle that Id1 and Id3 represent relevant targets in melanoma, and identify promising novel compounds with therapeutic potential that target Id1 and Id3.

BMP signaling is highly susceptible to extracellular regulation through the biochemical and physical properties of the ECM.[32] Here we introduce matrix-assisted autocrine signaling as an

additional mechanism through which the ECM can foster BMP signaling by suppressing diffusion of endogenously produced ligand. The diffusion coefficients we measured for BMP2 are similar to those reported for the Drosophila BMP homolog Dpp in vivo, where the diffusion coefficient of GFP-tagged Dpp in the wing imaginal disc was reported as $0.10 \pm 0.05\ \mu m^2\ s^{-1}$.[38] This is comparable to the diffusion coefficient of the slow species we observed for labelled BMP2 in Matrigel ($0.25 \pm 0.03\ \mu m^2\ s^{-1}$), and suggests that transient interactions with ECM components also reduce BMP mobility in vivo. The obtained diffusion coefficient of $96.3 \pm 0.9\ \mu m^2\ s^{-1}$ for BMP2 in bulk medium is in good agreement with published diffusion coefficients of proteins with similar size and under comparable conditions.[39]

Matrix-assisted autocrine signaling could conceivably not only foster BMP signaling, but may also be operative in any situation where cells express receptors for particular growth factors or cytokines, but produce only low levels of the cognate ligands that do not normally suffice to trigger the receptor in an autocrine manner. If a particular ECM environment substantially inhibits free diffusion of the ligand, then increased pericellular levels of the ligand could develop that ultimately reach the concentration required to activate the receptor, triggering autocrine stimulation.

Our data support the notion that matrix-assisted autocrine signaling fosters BMP-induced expression of Id1 and Id3, leading to increased tumorigenicity of melanoma cells. In the model systems analyzed, BMP4 and BMP7 were expressed at low levels by the melanoma cells, and were implicated in mediating the matrix-assisted autocrine signaling. For example noggin, which has the strongest binding affinity for BMP2, BMP4, and BMP7,[30,40] suppressed matrix-induced Id1 and Id3 expression. These data therefore suggest that BMP4 and BMP7 may be instrumental in determining tumorigenicity in melanoma cells. Consistent with this notion, BMP4 and BMP7 expression is upregulated in melanoma compared to nevi,[41] and BMP7 expression correlates with more aggressive melanoma cell phenotypes.[41,42]

Increased Id1 and Id3 expression may be relevant not only in the context of melanoma initiation, but also during invasion and metastasis. Notably, culture in 3D Matrigel increased outgrowth and invasiveness of melanoma cells in an Id1/Id3-dependent manner. Consistently, Id1 has been reported to be upregulated in metastatic melanoma.[23] Furthermore, while other tumors often respond with inhibition of migration or invasion to BMP treatment,[43–45] melanoma cells generally show enhanced migration and invasion following BMP stimulation.[41,46,47] Moreover, BMP ligands are more highly expressed in advanced stage melanomas, and are often secreted by melanoma cells themselves.[41,46] Thus during metastasis, the ECM constituents that disseminated tumor cells encounter when intravasating into a new organ microenvironment may be decisive in supporting tumor cells, for example through matrix-assisted autocrine BMP signaling, allowing the cells to survive and form metastases.

We also observed here that breast cancer cells increase Id1 and Id3 expression in 3D ECM environments. This suggests that therapeutic targeting of Id1 and Id3, which is upregulated in the cancer context through either matrix-assisted autocrine regulation or through other mechanisms, may be more broadly applicable across different tumor types. Cancer entities reported to exhibit increased Id1 and/or Id3 levels that correlate with poor survival include prostate cancer,[48] B-acute lymphoblastic leukemia,[49] non-small cell lung cancer,[50] ovarian cancer,[51] esophageal squamous cell carcinoma,[52] and breast cancer.[53] In many cases, Id1 and Id3 are co-expressed in tumor tissues. Given the evidence that Id1 and Id3 can compensate for each other,[24] their simultaneous targeting is likely to be beneficial, as suggested by the more robust reduction of tumor growth seen with the Id1/Id3 double knockout cells, compared to Id1 or Id3 single knockouts. Furthermore, as Id1 and Id3 are upregulated in response to vemurafenib, and mediate adaptive resistance in melanoma cells to vemurafenib treatment,[54] targeting Id1 and Id3 may prevent melanoma cells from developing adaptive resistance. The elevated BMP2 transcription observed in melanoma patients treated with BRAF or MEK inhibitors[46] could also potentially result in elevated expression of the BMP2 target genes Id1 or Id3. Indeed, we detected markedly higher levels of ID1 and ID3 expression in human melanoma lines with an invasive phenotype, which has been shown to be more resistant to RAF/MEK inhibitors.[36] These observations suggest that combining inhibitors of Id1 and Id3 with BRAF or MEK inhibitors in melanoma treatment may provide benefit for patients.

While the expression of Id1 and Id3 is not limited to tumor tissue, the fact that their loss potently suppressed tumor growth can offer a therapeutic window for their inhibition as cancer drug targets. Indeed, while the X6632 compound had a strong effect on tumor growth, we did not observe any adverse side effects from the treatment. The lack of in vivo toxicity may reflect the fact that although Id1 and Id3 proteins play a role in regulating the self-renewal and pluripotency of adult stem cells, they are mostly required in this context in response to injury.[55,56] It should also be noted that apart from the direct impact of Id1/Id3 targeting on tumor cells, the inhibition of Id1/Id3 in non-neoplastic tissues may actually augment the anti-cancer effects through regulating the tumor microenvironment. Id1 and Id3 have been implicated in the induction of angiogenesis,[57] lymphangiogenesis,[58] and in determining the differentiation status of tumor-promoting immune components such as myeloid-derived suppressor cells[59] and $Foxp3^+$ T_{reg} cells.[60] Inhibition of Id1 and Id3 may therefore suppress tumor growth and progression not only by direct effects on tumor cells, but also through preventing the creation of a protumorigenic microenvironment.

A number of tools have been developed for inhibiting Id1 or Id3 expression experimentally. Peptide-based approaches have been used, but difficulties in delivering the molecule to target cells and the pharmacological properties of the substances limit their efficacy.[61,62] Small molecule inhibitors and natural products that target Id1 or Id3 have also been described, but are rather unspecific.[63,64] CBD partially inhibits Id1 expression at the transcriptional level[37] and has anti-cancer properties,[65–67] but regulates the expression of other genes apart from Id1.[68,69] In comparison to these approaches, the novel inhibitors of Id1 and Id3 we report here offer considerable potential therapeutic advantages, both in terms of potency, anti-cancer efficacy, concomitant dual inhibition of Id1 and Id3, and lack of observable side effects. Future work will focus on investigating the therapeutic potential of these compounds.

4. Conclusion

Our study demonstrates that particular ECM environments can increase tumor initiation and growth through matrix-assisted autocrine BMP signaling, which upregulates expression of the transcriptional regulators Id1 and Id3. Id1 and Id3 are key mediators of matrix-regulated tumorigenesis, as their ablation in melanoma cells led to decreased growth and invasion in 3D matrix environments, and strongly impaired tumorigenesis in animal melanoma models. Importantly, this study identified a novel class of coumarin derivatives that inhibit Id1 and Id3 expression and suppress melanoma initiation and growth in vivo. These compounds represent promising leads for anti-cancer drug development.

5. Experimental Section

Cell Lines: The murine melanoma cell lines B16-F10 [70] and Ret [71] were cultured in DMEM or RPMI medium containing 10% FCS, 1% penicillin/streptomycin, respectively. The murine breast cancer cell line 4T1 [72] was cultured in DMEM containing 10% FCS, 1% penicillin/streptomycin. Cells were incubated at 37 °C and 5% CO_2 at maximal humidity in a cell culture incubator. 3D cultures were incubated in low-attachment poly-HEMA coated wells. Cells were regularly tested for mycoplasma infection using the VenorGeM Mycoplasma PCR Detection Kit (11-1250, Minerva Biolabs)

Collagen I Isolation from Mouse and Rat Tails: Mouse or rat tails were briefly rinsed with 70% EtOH, skin was removed and collagen fibers were cut into pieces and collected in PBS. After removing residual blood vessels, cartilage and muscle, collagen fibers were air dried and dissolved in 0.1% acetic acid at 4 °C, filtered through glass wool, then lyophilized and redissolved at an appropriate concentration in 0.1% acetic acid.

3D Cell Culture: For 3D cultures, cells were embedded in Matrigel HC (5 mg mL^{-1} or 10 mg mL^{-1}; 354 262, Corning Inc), Matrigel Growth Factor Reduced (GFR, 5 mg mL^{-1}), laminin I (4.5 mg mL^{-1}; 3446-005-01, Trevigen), collagen type I (4 mg mL^{-1}; isolated from rat/mouse tails, mixed with HBSS buffer and $NaHCO_3$ (7:1:1 v/v/v) and neutralized with NaOH), 0.75% alginate (180 947, Sigma Aldrich) in MOPS buffer (10×10^{-3} M MOPS, 0.85% NaCl, pH 7.2) and subsequently seeded into a poly-HEMA-coated well. Polymerization of the gels was performed for 30 min (Matrigel HC, collagen I) or 3 h (laminin I) at 37 °C. Alginate gels were crosslinked by addition of a polymerization solution (10×10^{-3} M MOPS, 100×10^{-3} M $CaCl_2$, pH 7.2) at room temperature for 5 min. After polymerization, gels were carefully overlaid with growth medium. Cells were cultured for 72 h prior to analysis. The following recombinant proteins and small molecule inhibitors were used for blocking experiments: recombinant noggin (120-10C, Peprotech), LDN-193 189 trihydrochloride (1509, Axon Medchem) and SB-431 542 (S1067, SelleckChem).

Tumor Growth and Initiation In Vivo: Mice were kept in groups of 4 in type III macrolon filtertop cages (Tecniplast, Hohenpeißenberg, Germany) containing SAFE fs14 bedding (Rettenmaier & Söhne, Rosenberg, Germany). Rat/mouse extruded food (SSNIFF, Soest, Germany) and sterilized water acidified with HCl (pH: 2.8–3.1) was provided ad libitum. The specific-pathogen-free area was kept at 20 °C and 30–60% humidity on a 7:00–20:00 light cycle. The health status of the animals in the facility was routinely assessed by a commercial veterinarian laboratory (mfd Diagnostics, Wendelsheim, Germany) through serological examinations every three months (epizootic diarrhoea of infant mice, mouse hepatitis virus, murine norovirus, minute virus of mice, Theiler´s encephalomyelitis virus, *Pasteurella pneumotropica*) or annually (*Clostridium piliforme*, Mousepox, lymphocytic choriomeningitis virus, mouse adenovirus type 1 and type 2, *Mycoplasma pulmonis*, pneumonia virus of mice, Reovirus type 3, Sendai virus). The serology was found to be negative for the parameters tested. In-house bred C57BL/6J mice aged 8–12 weeks were randomly allocated into experimental groups. Co-injection experiments with Id1/Id3 KO cells were performed with equal numbers of female and male mice in each group. For compound treatments only female mice were taken into the experiments. Group sizes were calculated using Fisher´s test (alpha = 5%, power = 80%). Cells were harvested using trypsin/EDTA and washed in PBS. The indicated numbers of living melanoma cells were subcutaneously injected into the flank of syngeneic mice in 100 µL PBS. For co-injection experiments, the indicated number of living cells was resuspended in 100 µL Matrigel HC (10 mg mL^{-1}; BD Biosciences), laminin I (4.5 mg mL^{-1}; Trevigen), collagen I (3.4 mg mL^{-1}) or fibronectin (625 µg mL^{-1}; Biopur), and subcutaneously injected into the flank of syngeneic mice. Tumor volume was calculated using the formula $4/3\pi$ ($d_1/2 \times d_2/2 \times d_3/2$), where d_1–d_3 represents the diameter of the tumor in three dimensions. Tumor initiating cell (TIC) frequency and *p*-values were calculated using ELDA software.[68] For drug treatments, CBD or X6632 were dissolved in DMSO, then injected intraperitoneally in a volume of 30 µL and at a dose of 18 mg kg^{-1} for the first 14 days following injection of the melanoma cells. Animal experiments were performed according to German legal requirements and were approved by the local regulatory authorities (approval numbers AZ 35–9185.81/G-83/04, AZ 35–9185.81/G-6/10, AZ 35–9185.81/G-45/16, AZ 35–9185.81/G-301/16).

Microarray Analysis: Gene expression profiles of B16-F10 and Ret melanoma cells cultured in 3D laminin I were compared to cells cultured as a monolayers on normal tissue culture plastic (2D), or as spheroids in methylcellulose-containing medium (3D MC) as previously described.[73] All conditions were analyzed in biological triplicates. RNA was isolated using TRIzol (Life technologies) according to the manufacturer's instructions. Further RNA processing, microarray analysis, bioinformatic analysis and quality control of the data was performed at Institut Curie, Paris (Translational Research Department, Affymetrix Platform) using MOE430 2.0 Arrays.

RNA Isolation and qRT-PCR: Cells were harvested for RNA isolation by directly adding TRIzol (Thermo Fisher Scientific) to the cells monolayer or cells embedded in 3D matrices. RNA was subsequently isolated according to the manufacturer's instructions. RNA (1–5 µg) was incubated with DNaseI (1–5 U; Thermo Fisher Scientific) for 30 min at 37 °C. DNaseI was inactivated by addition of EDTA and incubation at 65 °C for 10 min. cDNA was synthesized using reverse transcriptase (Thermo Fisher Scientific). Negative controls lacking reverse transcriptase were prepared for each sample to confirm successful DNAse treatment. Quantitative RT-PCR (qRT-PCR) was performed using SYBR Green mix (Applied Biosystems) on the OneStep Plus Realtime-PCR System (Applied Biosystems) or MX3005P (Stratagene) for 40 cycles with the following PCR conditions: 15 s 95 °C, 1 min 60 °C, 1 in 72 °C. Data were normalized to Rplp0, and relative expression of the target genes was determined using the ΔΔCt method. A list of primers can be found in Table S5 (Supporting Information).

Western Blot: Western blot analysis was performed as previously described.[74] Proteins in cell culture conditioned medium were concentrated using StrataClean Resin beads (Agilent) for 2 h at 4 °C under rotation prior to Western blotting. The following primary antibodies were used to detect specific proteins: Id1 (195-14, CalBioreagents), Id3 (17-3, CalBioreagents), phospho-Smad1 (13820S, Cell Signaling), Smad1 (9743S, Cell Signaling), β-actin (AC-15, Sigma Aldrich), vinculin (VIN-11-5, Sigma Aldrich), BMP4 (MAB1049, EMD Millipore) and BMP7 (500-P198, Peprotech). Protein bands were detected using HRP-conjugated secondary antibodies (P0447, P0448, Agilent Technologies) and enhanced chemiluminescence (32 106, Thermo Fisher Scientific).

CRISPR/Cas9: Generation of Id1/Id3 KO clones was performed as previously reported.[74] In short, cells were co-transfected with a gRNA vector, hCas9 plasmid[75] and sequence-specific single stranded donor oligonucleotides using Lipofectamin2000 reagent according to the manufacturer's protocol. Single cell clones were expanded and screened for alterations in genomic DNA sequences of the Id1 and Id3 genes with sequence-specific primers. Colonies with alterations in the genomic DNA sequences were selected and checked for Id1/Id3 protein expression by Western blot analysis. Colonies lacking a specific band for the Id1/Id3 protein were selected, seeded as single cells in 96-wells and subsequently analyzed for genomic alterations and the loss of Id1 and Id3 protein expression. Single cell clones obtained from the parental cell line were used as

controls. The sequences of vectors, oligonucleotides and primers used for CRISPR/Cas9 ablation of the Id1 and Id3 genes are summarized in Table S6 (Supporting Information).

3D Matrigel Assay: Cells (2×10^3) were mixed with Matrigel to obtain 150 µL of a cell/Matrigel (10 mg mL^{-1}) solution, which was seeded into a well of a 48-well plate. The gel was allowed to solidify at 37 °C for 30 min and was subsequently overlaid with complete growth medium (500 µL). After six days of culture, images were captured using a Leica DMI6000 B microscope at six different *x*/*y* positions in every well, and a minimum of five horizontal layers (*z* levels) at each position in order to get every colony in focus. Image analysis was performed using Fiji software.[76] Colonies were masked using the wand tool and the perimeter and area for all colonies with a minimum pixels size of 1500 were measured. An invasion index [77] was calculated as follows: Invasion index = $(\text{perimeter})^2/\text{area}$, resulting in a dimensionless measure of invasiveness.

Proliferation Assay in 2D: Cells were incubated for 72 h in 96-well plates and DNA content (as a measure of cell proliferation) was analyzed using the CyQUANT proliferation assay (C35006, Thermo Fisher Scientific). Growth medium was removed and 50 µL of CyQUANT dye diluted 1:500 in 1x HBSS was added per well. Plates were incubated for 15 min at 37 °C to allow the CyQUANT dye to incorporate into DNA. Fluorescence was measured by excitation at 485 nm and detection of emission at 530 nm, at 25 positions in each well using a Tecan Infinite M200 reader.

ELISA: To determine the concentration secreted of BMP4 and BMP7, melanoma cells were cultured in serum-free medium with 1% penicillin/streptomycin and 2% B27 supplement (Invitrogen, Darmstadt, Germany) for 48 h. The conditioned medium was harvested, centrifuged to clear cell debris and directly analyzed using the BMP4 (ABIN1371421, antibodies-online) or BMP7 ELISA Kit (ABIN365657, antibodies-online) according to the manufacturer's instructions.

Immunofluorescence Staining and Confocal Microscopy: Cells were cultured in 3D Matrigel (10 mg mL^{-1}) for 72 h. The cell/Matrigel plug was fixed with 2% PFA / 0.1% glutaraldehyde for 30 min, then washed extensively with 0.1 M glycine in PBS. The plug was transferred to a 50 mL Falcon tube with 20% sucrose in PBS and allowed to sink to the bottom of the tube at 4 °C for 3–4 days. The plug was then embedded in Tissue-Tek O.C.T. compound and frozen at −80 °C. Cryosections (20 µm) were cut and air-dried on a glass slide. For immunofluorescence staining, cryosections were hydrated in PBS for 1 h. Blocking was performed using the blocking solution supplied with the M.O.M. Kit (BMK-2202, Vector labs) overnight at 4 °C. The next day, the samples were incubated in antibodies against BMP4 (500-M121, Peprotech) or mouse IgG isotype control (sc-2025, Santa Cruz) over two nights at 4 °C. After washing with PBS, secondary antibodies against mouse IgG (#A-11003, Thermo Fisher Scientific) were applied over night at 4 °C. After washing with PBS, slides were mounted with DAPI Fluoromount-G (0100-20, SouthernBiotech). Confocal microscopy images were obtained using a Leica SP5 MP (LIMA core facility, Medical Faculty Mannheim, University of Heidelberg). Image analysis was performed using Fiji.[76]

Fluorescence Correlation Spectroscopy: Recombinant human BMP2 protein (BioVision, Milpitas, USA) was labeled using the Alexa Fluor 555 Microscale Protein Labeling Kit (A30007, Thermo Fisher Scientific) according to the manufacturer's protocol. The degree of labeling was calculated to be ~4.5 Alexa555 molecules/BMP2 dimer. The labeled BMP2 was dialyzed using the Slide-A-Lyzer Dialysis cassette with molecular weight cutoff of 10 kDa (66 380, Thermo Fisher Scientific). The dialyzed BMP2 was stored at −20 °C with BSA as stabilizer, and protected from light.

BMP2 mobility in Matrigel, laminin, RPMI growth medium and RPMI supplemented with 10 mg mL^{-1} bovine serum albumin (Sigma-Aldrich) was determined by fluorescence correlation spectroscopy using a SP5 confocal scanning microscope (Leica) equipped with a 63x water immersion objective (HCX PL APO CS, Leica) and a pulsed white light laser (SuperK, Koheras). Time-correlated single photon streams were recorded using two fiber-coupled avalanche photo diodes (APDs, SPCM AQR-14 PerkinElmer) connected to a Hydraharp 300 time-correlated single photon counting (TCSPC) system via a PHR800 router (both PicoQuant) for recording time-correlated single photon data streams. The white light laser was operated at 80 MHz pulse repetition rate and a wavelength of 540 nm was selected for excitation of Alexa555. An excitation intensity of 4 µW, well below the saturation intensity of Alexa555, was used for all measurements. Emitted fluorescence was spectrally filtered with a 585/65 nm bandpass filter and distributed onto both APDs using a 50/50 beam splitter. Measurements were performed for 180 seconds per data point, at a distance of 10 µm from the coverslip surface, and at 26 °C.

Samples were prepared in LabTek chambered coverslips (Nunc) using RPMI (Gibco) to dilute gels and Alexa555-labeled BMP2. Alexa555-labeled BMP2 (20×10^{-9} M protein), laminin (4.5 mg mL^{-1}) or Matrigel (10 mg mL^{-1}) were mixed extensively and incubated at 37 °C for at least 1 h. Prior to measurements, pre-incubated samples were equilibrated at room temperature for at least 30 min before starting data acquisition.

Raw TCSPC data was acquired and correlated using the SymPhoTime software package (PicoQuant). Correlations were computed as cross-correlation of the signals recorded by the two APDs for lag times from 0.1 µs to 10 s. Correlated data was fitted with models including one or two species with free 3D diffusion and a triplet fraction to account for observed blinking of Alexa555. All fits were performed using PyCorrFit.[78] The effective observation volume (V_{eff}) of the setup was calibrated using the published diffusion coefficient for rhodamine B of 427 $\mu m^2\ s^{-1}$ in aqueous solution at 25 °C.[79] Typical for V_{eff} were 0.22 fL with a structural parameter (beam $waist_z/waist_{xy}$) *K* around 5.5. Measurements were fit individually with fixed values for triplet time of BMP2-conjugated Alexa555 (3.9 µs determined from an unrestricted fit of BMP2/RPMI data), and structural parameter (5.5, determined from rhodamine B calibration measurements). Raw and fitted data was averaged using custom-written routines in Matlab (MathWorks).

Bioinformatic Analysis: Gene expression data (RNA-Seq V2 RSEM) for tumor and normal tissue from the cutaneous melanoma cohort of The Cancer Genome Atlas (TCGA SKCM, Firehose Legacy; 472 samples with mRNA data), were downloaded from the National Cancer Institute GDC Data Portal and the cBio Portal.[80,81] The list of genes coding for ECM structural components (Table S4 (Supporting Information), a total of 100 genes) was assembled based on a survey of the literature and searches of the NCBI Gene database. A random set of control genes (Table S4, Supporting Information) was assembled from the first 100 genes along human chromosome 1, for which mRNA expression data were available for the TCGA cutaneous melanoma cohort. For analysis of gene expression in human melanoma cell lines with proliferative and invasive phenotypes the Melanoma Phenotype-Specific Expression (MPSE) facility of the Heuristic Online Phenotype Prediction (HOPP) tool[34] was used.

Synthetic Route toward Shown Coumarin Compounds: KHMDS, THF, dibromo alkane, −16 °C to r.t., 16 h, 78%; b) DIBAL-H, DCM, −78 °C, 1 h, 92%; c) 1) *n*-propyl triphenyl phosphonium bromide, KHMDS, THF, 0 °C to 10 °C, 30 min, 2) starting material, 10 °C, 1 h, 99%; d) Pd/C, H_2-atmosphere, ethyl acetate, 24 h, 97%; e) 1.) TMEDA, diethyl ether, 0 °C, n-BuLi, 2 h, r.t., 2.) 0 °C, DMF, 4 h, r.t., 91%; f) $AlCl_3$, NaI, ACN, DCM, 1.5 h, r.t., 80%; g) hexanoic acid anhydride, K_2CO_3, microwave irradiation (180 °C, 65 min, 300 W), 82%; h) BBr_3 in CH_2Cl_2 (5.00 equiv.), CH_2Cl_2, −78 °C – rt (30 min), 92% (Figure S5B, Supporting Information).

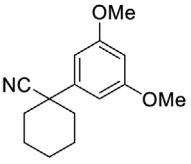

Synthesis of Compound X6632—1-(3,5-Dimethoxyphenyl)cyclohexane-1-carbonitrile: KHMDS (25.3 g; 127 mmol, 3.00 equiv.) was added to a solution of 2-(3,5-dimethoxyphenyl)acetonitrile (7.50 g; 42.3 mmol, 1.00 equiv.) in abs. tetrahydrofuran (200 mL) under argon counterflow at −16 °C. The mixture was stirred for 3 min at the same temperature and then 1,4-dibromopentane (6.24 mL; 10.6 g, 46.6 mmol, 1.10 equiv.), diluted in abs. tetrahydrofuran (50 mL), was added dropwise. The mixture was allowed to warm to room temperature and stirred overnight. The reaction was quenched via the addition of ammonium chloride solution (150 mL) and diluted with 100 mL of diethyl ether. The organic layers were extracted with diethyl ether (3 × 200 mL) and the combined organic layers were dried over sodium sulfate. Removal of the volatiles under reduced pressure and purification via flash column chromatography (CH/EtOAc 5:1) resulted in 8.09 g (78%) of the pure product as a colorless oil. Analytical data are

consistent with the literature.[82] Rf (CH/EtOAc 5:1): 0.43; ^{1}H NMR (300 MHz, $CDCl_3$): $\delta = 6.63$ (d, $J = 2.2$ Hz, 2H, 2 × HAr), 6.40 (t, $J = 2.2$ Hz, 1H, HAr), 3.81 (s, 6H, 2 × OCH_3), 2.21–2.16 (m, 2H, CH_2), 1.93–1.65 (m, 6H, CH_2), 1.46–1.02 (m, 2H, CH_2) ppm.

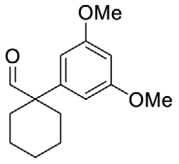

Synthesis of Compound X6632—1-(3,5-Dimethoxyphenyl)cyclohexane-1-carbaldehyde: A solution of 1-(3,5-dimethoxyphenyl)cyclohexane-1-carbonitrile (7.97 g; 32.5 mmol, 1.00 equiv.) in abs. dichloromethane (250 mL) under argon atmosphere was cooled to −78 °C and DIBAL-H (81.2 mL; 1 m in dichloromethane, 81.2 mmol, 2.50 equiv.) was added dropwise. The mixture was stirred for an additional 1 h at the same temperature and the reaction was then quenched by dropwise addition of 10% aqueous sodium potassium-tartrate (120 mL). After thawing up to room temperature the mixture was stirred for another 40 min and the aqueous layer extracted with ethyl acetate (3 × 200 mL). The combined organic layers were washed with brine (300 mL) and dried over sodium sulfate. Removal of the volatiles under reduced pressure and purification via flash column chromatography (CH/EtOAc 10:1) resulted in 7.39 g (92%) of the pure product as a colorless oil. Analytical data are consistent with the literature.[83] Rf (CH/EtOAc 20:1): 0.20; ^{1}H NMR (300 MHz, $CDCl_3$): δ = 9.34 (s, 1H, CHO), 6.46 (d, J = 2.2 Hz, 2H, 2 × HAr), 6.37 (t, J = 2.2 Hz, 1H, HAr), 3.78 (s, 6H, 2 × OCH_3), 2.27–2.22 (m, 2H, CH_2), 1.85–1.78 (m, 2H, CH_2), 1.69–1.57 (m, 3H, CH_2), 1.52–1.25 (m, 3H, CH2) ppm.

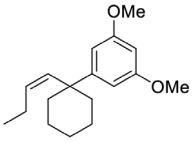

Synthesis of Compound X6632—(Z)-1-(1-(But-1-en-1-yl)cyclohexyl)-3,5-dimethoxybenzene: KHMDS (18.8 g; 94.3 mmol, 3.00 equiv.) was added to a suspension of *n*-propyl triphenylphosphonium bromide (36.3 g; 94.3 mmol, 3.00 equiv.) in abs. tetrahydrofuran (300 mL) at 0 °C, under argon counterflow. The mixture was stirred for 30 min at 10 °C and a solution of 1-(3,5-dimethoxyphenyl)cyclohexane-1-carbaldehyde (7.81 g; 33.7 mmol, 1.00 equiv.) in abs. tetrahydrofuran (50 mL) was added dropwise. After stirring for another 60 min the reaction was quenched by the addition of ammonium chloride solution (200 mL). The aqueous layer was extracted with diethyl ether (3 × 200 mL) and the combined organic layers were dried over sodium sulfate. Removal of the volatiles under reduced pressure and purification via flash column chromatography (CH/EtOAc 10:1) resulted in 8.62 g (99%) of the pure product as a colorless oil. Analytical data are consistent with the literature.[83] Rf (CH/EtOAc 5:1): 0.65. ^{1}H NMR (300 MHz, $CDCl_3$): δ = 6.58 (d, J = 2.3 Hz, 2H, 2 × HAr), 6.28 (t, J = 2.3 Hz, 1H, HAr), 5.63 (dt, J = 11.2 Hz, J = 1.7 Hz, 1H, HDB), 5.34 (dt, J = 11.2 Hz, J = 7.4 Hz, 1H, HDB), 3.78 (s, 6H, 2 × OCH_3), 1.95–1.90 (m, 2H, CH_2), 1.72–1.56 (m, 9H, CH_2), 1.31–1.24 (m, 1H, CH_2), 0.72 (t, J = 7.5 Hz, 3H, CH_3) ppm.

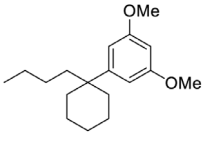

Synthesis of Compound X6632—1-(1-Butylcyclohexyl)-3,5-dimethoxybenzene: Palladium (1.73 g) on activated charcoal (10% Pd/C) was added to a solution of ((Z)-1-(1-(but-1-en-1-yl)cyclohexyl)-3,5-dimethoxybenzene (8.50 g) in ethyl acetate. Hydrogen gas was bubbled through the solution for several hours and subsequently kept under hydrogen atmosphere for 24 h. Filtration through Celite, rinsing with ethyl acetate and removal of the volatiles resulted in 8.31 g (97%) of the pure product as a colorless oil. Analytical data are consistent with the literature.[83] Rf (CH/EtOAc 5:1): 0.68. ^{1}H NMR (300 MHz, $CDCl_3$): δ = 6.48 (d, J = 2.3 Hz, 2H, 2 × HAr), 6.3 (t, J = 2.3 Hz, 1H, HAr), 3.80 (s, 6H, 2 × OCH_3), 2.02–1.98 (m, 2H, CH_2), 1.57–1.36 (m, 10H, 5 × CH_2), 1.18–1.09 (m, 2H, CH_2), 0.96–0.88 (m, 2H, CH_2), 0.78 (t, J = 7.3 Hz, 3H, CH_3) ppm.

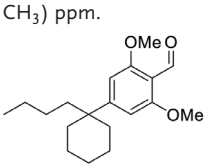

Synthesis of Compound X6632—4-(1-Butylcyclohexyl)-2,6-dimethoxybenzaldehyde: 1-(1-butylcyclohexyl)-3,5-dimethoxybenzene (8.26 g; 29.9 mmol, 1.00 equiv.) was dissolved in diethyl ether (60 mL), and TMEDA (6.72 mL; 5.21 g, 44.8 mmol, 1.50 equiv.) was added dropwise. The solution was cooled to 0 °C and *n*-butyl lithium (17.9 mL; 2.5 m in *n*-hexanes, 44.8 mmol, 1.50 equiv.) was added slowly. After stirring for 4 h at room temperature, the solution was cooled to 0 °C, dimethylformamide (6.89 mL; 6.551 g, 89.7 mmol, 3.00 equiv.) were added and the mixture was stirred for another 4 h at room temperature. The reaction was quenched by the addition of brine (60 mL) and extracted with diethyl ether (3 × 15 mL). The combined organic layers were dried over sodium sulfate, the volatiles were removed under reduced pressure and the residue was then purified via flash column chromatography (CH/EtOAc 10:1) to result in 8.31 g (91%) of the product as yellow oil that was used directly in the next step. Analytical data are consistent with the literature.[83] Rf (CH/ EtOAc 10:1): 0.19; ^{1}H NMR (300 MHz, $CDCl_3$): δ = 10.46 (s, 1H, CHO), 6.52 (s, 2H, 2 × HAr), 3.89 (s, 6H, 2 × OCH_3), 2.07–1.94 (m, 2H, CH_2), 1.66 – 1.33 (m, 10H, 5 × CH_2), 1.29–1.04 (m, 2H, CH_2), 1.01–0.85 (m, 2H, CH_2), 0.79 (t, J = 7.3 Hz, 3H, CH_3) ppm.

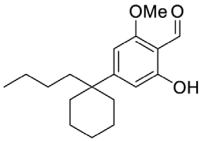

Synthesis of Compound X6632—4-(1-Butylcyclohexyl)-2-hydroxy-6-methoxybenzaldehyde: 4-(1-Butylcyclohexyl)-2,6-dimethoxybenzaldehyde (8.00 g; 1.00 eq, 26.3 mmol) was dissolved in a mixture of dry acetonitrile (100 mL) and dry dichloromethane (50 mL), cooled to 0 °C, and aluminum trichloride (8.76 g; 65.7 mmol, 2.50 eq,) and sodium iodide (9.85 g; 65.7 mmol, 2.50 eq,) were added slowly under argon counterflow. The reaction mixture was stirred for 1.5 h at room temperature, quenched with water, and extracted with dichloromethane (3 × 30 mL). The combined organic layers were then washed with sodium thiosulfate solution, dried over sodium sulfate and after removal of volatiles, the crude product was purified via flash column chromatography (CH/EtOAc 40:1) to result in 6.11 g (80%) of a yellow oil. Analytical data are consistent with the literature.[83] Rf (CH/EtOAc 40:1): 0.26; ^{1}H NMR (300 MHz, $CDCl_3$): δ = 11.92 (s, 1H, C2-OH), 10.26 (s, 1H, CHO), 6.51 (d, J = 1.3 Hz, 1H, HAr), 6.34 (d, J = 1.3 Hz, 1H HAr), 3.88 (s, 3H, OCH_3), 2.00–1.32 (m, 12H, 6 × CH_2), 1.20–1.10 (m, 2H, CH_2), 0.96–0.88 (m, 2H, CH_2), 0.79 (t, J = 7.3 Hz, 3H, CH_3) ppm.

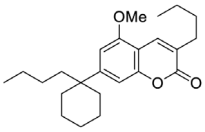

Synthesis of Compound X6632—7-(1-Butylcyclohexyl)-5-methoxy-3-butyl-2H-chromen-2-one: 4-(1-Butylcyclohexyl)-2-hydroxy-6-methoxybenzaldehyde (200 mg; 0.69 mmol, 1.00 equiv.), hexanoic acid anhydride (0.56 mL; 517 mg, 2.41 mmol, 3.50 equiv.) and potassium carbonate (4.8 mg; 270 µmol, 0.05 equiv.) were placed in a microwave vial and heated at 180 °C for 65 min at 300 W microwave irradiation. The resulting mixture was allowed to cool to room temperature, poured onto crushed ice and the pH was adjusted to ≈7 with sodium bicarbonate. The mixture was then extracted with ethyl acetate (3 × 50 mL) and the combined organic layers were dried over sodium sulfate. Removal of the volatiles under reduced pressure and purification via flash column chromatography (CH/EtOAc 100:1) resulted in 210 mg (82%) of an off-white solid. Rf (CH/EtOAc 50:1): 0.31; MP: 143.8 °C; ^{1}H NMR (400 MHz, $CDCl_3$): δ = 7.81 (s, 1H, 4-CH), 6.90–6.86 (m, 1H, HAr), 6.66 (d, J = 1.5 Hz, 1H, HAr), 3.92 (s, 3H, OCH_3), 2.55 (t, J = 7.7 Hz, 2H, CH_2), 2.11–1.94 (m, 2H, CH_2), 1.70–1.30 (m, 14H, 7 × CH_2), 1.13 (p, J = 7.3 Hz, 2H, CH_2), 1.00–0.85 (m, 5H, CH_2, CH_3), 0.77 (t, J = 7.3 Hz, 3H, CH_3) ppm; ^{13}C NMR (100 MHz, $CDCl_3$): δ = 162.4 (Cquart., COO), 155.4 (Cquart., CAr), 154.2 (Cquart., CAr), 152.4 (Cquart., CAr), 133.5 (+, 4-CArH), 127.2(Cquart., CAr), 108.0 (Cquart., CAr), 107.9 (+, CArH), 103.9 (+, CArH), 55.9 (+, OCH_3), 43.6(Cquart., CCH), 42.3 (–, CH_2), 36.5 (–, 2 × CH_2), 30.8 (–, CH_2), 30.5 (–, CH_2), 26.6 (–, CH_2), 25.8 (–, CH_2), 23.4 (–, CH_2), 22.6 (–, 2 × CH_2), 14.1 (+, CH_3), 14.0 (+, CH_3) ppm. – IR (KBr): $\tilde{\nu}$ = 2926 (m), 2854 (w), 1714 (m), 1613 (m), 1570 (w), 1495 (w), 1453 (m), 1413 (m), 1376 (w), 1344 (w), 1291 (w), 1245 (m), 1163 (w), 1104 (m), 1073 (w), 1044 (m), 991 (m), 943 (w), 906 (w), 834 (w), 798 (w), 760 (w), 712 (w), 684 (w), 653 (w), 558 (w), 494 (vw), 429 (vw) cm^{-1}; MS (70 eV, EI): m/z (%) = 370 (96) [M]+, 328 (7), 327 (8), 315 (10), 314 (45), 313 (100) [M – C_4H_9]+, 274 (6), 271 (5), 259 (5), 246 (10), 245 (54), 233 (19), 203 (7), 202 (11), 189 (5), 81 (7); HRMS ($C_{24}H_{34}O_3$): calc. 370.2502; found 370.2502; Elemental analysis: $C_{24}H_{34}O_3$: calc. C 77.80; H 9.25; found C 77.78, H 9.43.

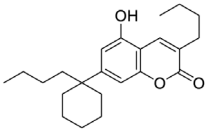

Synthesis of Compound X6632—7-(1-Butylcyclohexyl)-5-hydroxy-3-butyl-2H-chromen-2-one: 7-(1-Butylcyclohexyl)-5-methoxy-3-butyl-2H-chromen-2-one (116 mg; 356 µmol, 1.00 equiv.) was dissolved in dry dichloromethane (5 mL). The solution was cooled to −78 °C and boron tribromide (1.78 mL; 1 m in dichloromethane, 1.78 mmol, 5.00 equiv.) was added dropwise. The mixture was stirred for 30 min at this temperature and then allowed to warm to room temperature. The reaction was quenched after 16 h at 0 °C by addition of sodium bicarbonate. The aqueous layer was extracted with dichloromethane (3 × 15 mL) and the combined organic layers were washed with brine, dried over sodium sulfate and the volatiles were removed under reduced pressure. The crude product was then purified via flash column chromatography (CH/EtOAc 5:1) to give the product as 116 mg (92%) of a white solid. Rf (CH/EtOAc 5:1): 0.43. MP: 154.0 °C; ^{1}H NMR (400 MHz, $CDCl_3$): δ = 7.89 (s, 1H, 4-CH), 6.83 (d, J = 1.4 Hz, 1H, HAr), 6.73 (d, J = 1.5 Hz, 1H, HAr), 6.54 (s, 1H, OH), 2.70–2.48 (m, 2H, CH_2), 2.04–1.93 (m, 2H, CH_2), 1.68–1.58 (m, 2H, CH_2), 1.57–1.27 (m, 12H, 6 × CH_2), 1.17–1.05 (m, 2H, CH_2), 0.94 (t, J = 7.3 Hz, 3H, CH_3), 0.92–0.83 (m, 2H, CH_2), 0.75 (t, J = 7.3 Hz, 3H, CH_3) ppm. ^{13}C NMR (100 MHz, $CDCl_3$): δ = 163.3 (Cquart., COO), 154.3 (Cquart., CAr), 152.7 (Cquart., CAr), 152.2 (Cquart., CAr), 134.3 (+, 4-CArH), 126.8 (Cquart., CAr), 109.1 (+, CArH), 107.5 (+, CArH), 107.1 (Cquart., CAr), 43.8 (–, CH2), 42.0 (Cquart., CCH), 36.4 (–, 2 × CH_2), 30.7 (–, CH_2), 30.5 (–, CH_2), 26.6 (–, CH_2), 25.8 (–, CH_2), 23.4 (–, CH_2), 22.6 (–, CH_2), 22.5 (–, 2 × CH_2), 14.1 (+, CH_3), 14.0 (+, CH_3) ppm. – IR (KBr): $\tilde{\nu}$ = 3171 (w), 2925 (w), 2853 (w), 1670 (m), 1613 (m),1573 (w), 1451 (w), 1421 (m), 1345 (w), 1288 (w), 1253 (w), 1185 (w), 1124 (w), 1101 (w), 1066 (w), 939 (w), 862 (w), 842 (w), 782 (w), 745 (w), 728 (w), 608 (vw), 529 (w), 414 (vw) cm^{-1}; MS (70 eV, EI): m/z (%) = 356 (71) [M]+, 331 (8), 314 (12), 301 (8), 300 (46), 299 (100) [M – C_4H_9]+, 281 (8), 262 (7), 260 (9); HRMS ($C_{23}H_{32}O_3$): calc. 356.2346; found 356.2347; Elemental analysis: $C_{23}H_{32}O_3$: calc. C 77.49, H 9.05; found C 77.27, H 9.09.

Compound Library Screens: To screen the chemical library for compounds with an inhibitory effect on Id1 and Id3 expression, melanoma cells were simultaneously stimulated with BMP4 (10 ng mL^{-1}, 315–27, Peprotech) and treated with the substances at the indicated concentrations for 24 h. Treatment with CBD served as a reference. DMSO served as a solvent control. Effects on Id1 and Id3 expression levels were analyzed by Western blotting.

Statistical Analysis: Statistical analysis was performed using GraphPad Prism software. Comparison of two groups was performed using unpaired two-tailed Student's t-test. Multiple groups were compared using one-way ANOVA followed by Tukey's, Dunnett's and Fisher's least significant difference tests for multiple pairwise comparisons. Tumor initiating cell (TIC) frequency was analyzed using ELDA software.[84] Tumor growth curves were compared using nested ANOVA analysis with the help of the statistics department of the Medical Faculty Mannheim (Dr. Svetlana Hetjens and Prof. Christel Weiß). Graphs present means with error bars showing standard error of the mean (SEM). qPCR data were normalized to the mean of the control condition. The level of statistical significance was defined as * $p < 0.05$, ** $p < 0.01$, *** $p < 0.001$.

Supporting Information

Supporting Information is available from the Wiley Online Library or from the author.

Acknowledgements

This work was funded by the Deutsche Forschungsgemeinschaft (DFG, German Research Foundation)–Project number 259332240 / RTG 2099 (J.P.S. and G.S.), the Chinese Scholarship Council (R.W.) and the European Union (HEALTH-F2-2008-201662) under the auspices of the FP7 collaborative project TuMIC (J.P.S.). The authors acknowledge the DFG Core Facility MOLECULE ARCHIVE (Grant Numbers: BR1750/40-1, JU2909/5-1) for the management and provision of the compounds for screening, funding from the Deutsche Forschungsgemeinschaft, DFG, PhotoQuant HE4559/6-1 (K.Y and D.-P.H.) and Germany's Excellence Strategy2082/1390761711 (M.T. and S.B.). The authors gratefully acknowledge the expert technical assistance of the animal facility at the Institute of Biological and Chemical Systems (IBCS) at Karlsruhe Institute of Technology (KIT). The authors acknowledge the support of the Core Facility Live Cell Imaging Mannheim at the Centre for Biomedicine and Medical Technology Mannheim (CBTM) (DFG INST 91027/10-1 FUGG). The authors thank Karen Bieback and Susanne Elvers-Hornung from the Institute for Transfusion Medicine and Immunology Mannheim for access to the Tecan Infinite M200 reader and technical support. The authors thank Annette Gruber for excellent technical work.

Open access funding enabled and organized by Projekt DEAL.

Conflict of Interest

The authors declare no conflict of interest.

Keywords

bone morphogenetic proteins, coumarin derivatives, DNA binding inhibitors, extracellular matrix, melanoma

Received: April 2, 2020
Revised: July 10, 2020
Published online:

[1] P. B. Gupta, I. Pastushenko, A. Skibinski, C. Blanpain, C. Kuperwasser, *Cell Stem Cell* **2019**, *24*, 65.
[2] J. Varga, F. R. Greten, *Nat. Cell Biol.* **2017**, *19*, 1133.
[3] C. Frantz, K. M. Stewart, V. M. Weaver, *J. Cell Sci.* **2010**, *123*, 4195.
[4] R. Rakian, T. J. Block, S. M. Johnson, M. Marinkovic, J. Wu, Q. Dai, D. D. Dean, X.-D. Chen, *Stem Cell Res. Ther.* **2015**, *6*, 235.
[5] A. J. Engler, S. Sen, H. L. Sweeney, D. E. Discher, *Cell* **2006**, *126*, 677.
[6] F. Niola, X. Zhao, D. Singh, A. Castano, R. Sullivan, M. Lauria, H. Nam, Y. Zhuang, R. Benezra, D. Di Bernardo, A. Iavarone, A. Lasorella, *Nat. Cell Biol.* **2012**, *14*, 477.
[7] E. Quintana, M. Shackleton, M. S. Sabel, D. R. Fullen, T. M. Johnson, S. J. Morrison, *Nature* **2008**, *456*, 593.
[8] S. Kelderman, T. N. M. Schumacher, J. B. A. G. Haanen, *Mol. Oncol.* **2014**, *8*, 1132.
[9] J. M. Zaretsky, A. Garcia-Diaz, D. S. Shin, H. Escuin-Ordinas, W. Hugo, S. Hu-Lieskovan, D. Y. Torrejon, G. Abril-Rodriguez, S. Sandoval, L. Barthly, J. Saco, B. Homet Moreno, R. Mezzadra, B. Chmielowski, K. Ruchalski, I. P. Shintaku, P. J. Sanchez, C. Puig-Saus, G. Cherry, E. Seja, X. Kong, J. Pang, B. Berent-Maoz, B. Comin-Anduix, T. G. Graeber, P. C. Tumeh, T. N. M. Schumacher, R. S. Lo, A. Ribas, *N. Engl. J. Med.* **2016**, *375*, 819.
[10] W. Hugo, J. M. Zaretsky, L. Sun, C. Song, B. H. Moreno, S. Hu-Lieskovan, B. Berent-Maoz, J. Pang, B. Chmielowski, G. Cherry, E. Seja, S. Lomeli, X. Kong, M. C. Kelley, J. A. Sosman, D. B. Johnson, A. Ribas, R. S. Lo, *Cell* **2016**, *165*, 35.
[11] M. J. C. Hendrix, E. A. Seftor, A. R. Hess, R. E. B. Seftor, *Oncogene* **2003**, *22*, 3070.
[12] M. Hölzel, T. Tüting, *Trends Immunol.* **2016**, *37*, 364.
[13] S. Ghislin, F. Deshayes, J. Lauriol, S. Middendorp, I. Martins, R. Al-Daccak, C. Alcaide-Loridan, *Melanoma Res.* **2012**, *22*, 184.
[14] E. Quintana, M. Shackleton, H. R. Foster, D. R. Fullen, M. S. Sabel, T. M. Johnson, S. J. Morrison, *Cancer Cell* **2010**, *18*, 510.
[15] M. J. C. Hendrix, E. A. Seftor, D. A. Kirschmann, V. Quaranta, R. E. B. Seftor, *Ann. N. Y. Acad. Sci.* **2003**, *995*, 151.
[16] A. Hollnagel, *J. Biol. Chem.* **1999**, *274*, 19838.

[17] Y.-Y. Liang, F. C. Brunicardi, X. Lin, *Cell Res.* **2009**, *19*, 140.
[18] X. H. Sun, N. G. Copeland, N. A. Jenkins, D. Baltimore, *Mol. Cell. Biol.* **1991**, *11*, 5603.
[19] G. P. Gupta, J. Perk, S. Acharyya, P. de Candia, V. Mittal, K. Todorova-Manova, W. L. Gerald, E. Brogi, R. Benezra, J. Massagué, *Proc. Natl. Acad. Sci. USA* **2007**, *104*, 19506.
[20] C. A. O'Brien, A. Kreso, P. Ryan, K. G. Hermans, L. Gibson, Y. Wang, A. Tsatsanis, S. Gallinger, J. E. Dick, *Cancer Cell* **2012**, *21*, 777.
[21] X. Lai, J. Liao, W. Lin, C. Huang, J. Li, J. Lin, Q. Chen, Y. Ye, *Oncol. Rep.* **2014**, *32*, 79.
[22] C. Roschger, C. Cabrele, *Cell Commun. Signaling* **2017**, *15*, 7.
[23] O. Straume, L. A. Akslen, *Br. J. Cancer* **2005**, *93*, 933.
[24] L. Pan, S. Sato, J. P. Frederick, X. H. Sun, Y. Zhuang, *Mol. Cell. Biol.* **1999**, *19*, 5969.
[25] R. Fridman, G. Benton, I. Aranoutova, H. K. Kleinman, R. D. Bonfil, *Nat. Protoc.* **2012**, *7*, 1138.
[26] A. Hata, G. Lagna, J. Massagué, A. Hemmati-Brivanlou, *Genes Dev.* **1998**, *12*, 186.
[27] T. Imamura, M. Takase, A. Nishihara, E. Oeda, J. Hanai, M. Kawabata, K. Miyazono, *Nature* **1997**, *389*, 622.
[28] S.-H. Hong, J. B. J.-H. Lee, J. B. J.-H. Lee, J. Ji, M. Bhatia, *J. Cell Sci.* **2011**, *124*, 1445.
[29] G. D. Cuny, P. B. Yu, J. K. Laha, X. Xing, J.-F. Liu, C. S. Lai, D. Y. Deng, C. Sachidanandan, K. D. Bloch, R. T. Peterson, *Bioorg. Med. Chem. Lett.* **2008**, *18*, 4388.
[30] L. B. Zimmerman, J. M. De Jesús-Escobar, R. M. Harland, *Cell* **1996**, *86*, 599.
[31] S. K. Halder, R. D. Beauchamp, P. K. Datta, *Neoplasia* **2005**, *7*, 509.
[32] G. Sedlmeier, J. P. Sleeman, *Biochem. Soc. Trans.* **2017**, *45*, 173.
[33] K. Y. Lee, D. J. Mooney, *Prog. Polym. Sci.* **2012**, *37*, 106.
[34] D. S. Widmer, P. F. Cheng, O. M. Eichhoff, B. C. Belloni, M. C. Zipser, N. C. Schlegel, D. Javelaud, A. Mauviel, R. Dummer, K. S. Hoek, *Pigm. Cell Melanoma Res.* **2012**, *25*, 343.
[35] K. S. Hoek, N. C. Schlegel, P. Brafford, A. Sucker, S. Ugurel, R. Kumar, B. L. Weber, K. L. Nathanson, D. J. Phillips, M. Herlyn, D. Schadendorf, R. Dummer, *Pigm. Cell Res.* **2006**, *19*, 290.
[36] M. C. Zipser, O. M. Eichhoff, D. S. Widmer, N. C. Schlegel, N. L. Schoenewolf, D. Stuart, W. Liu, H. Gardner, P. D. Smith, P. Nuciforo, R. Dummer, K. S. Hoek, *Pigm. Cell Melanoma Res.* **2011**, *24*, 326.
[37] S. D. McAllister, R. T. Christian, M. P. Horowitz, A. Garcia, P.-Y. Desprez, *Mol. Cancer Ther.* **2007**, *6*, 2921.
[38] A. Kicheva, P. Pantazis, T. Bollenbach, Y. Kalaidzidis, T. Bittig, F. Jülicher, M. González-Gaitán, *Science* **2007**, *315*, 521.
[39] Z. Petrásek, P. Schwille, *Biophys. J.* **2008**, *94*, 1437.
[40] J. Groppe, J. Greenwald, E. Wiater, J. Rodriguez-Leon, A. N. Economides, W. Kwiatkowski, M. Affolter, W. W. Vale, J. C. I. Belmonte, S. Choe, *Nature* **2002**, *420*, 636.
[41] T. Rothhammer, I. Poser, F. Soncin, F. Bataille, M. Moser, A.-K. Bosserhoff, *Cancer Res.* **2005**, *65*, 448.
[42] M.-Y. Hsu, S. Rovinsky, S. Penmatcha, M. Herlyn, D. Muirhead, *Cancer Metastasis Rev.* **2005**, *24*, 251.
[43] L. Wang, P. Park, H. Zhang, F. La Marca, A. Claeson, J. Valdivia, C.-Y. Lin, *Cancer Biol. Ther.* **2011**, *11*, 457.
[44] L. Ye, H. Kynaston, W. G. Jiang, *J. Urol.* **2009**, *181*, 2749.
[45] C. Wang, F. Hu, S. Guo, D. Mi, W. Shen, J. Zhang, Y. Qiao, T. Zhu, S. Yang, *J. Cancer Res. Clin. Oncol.* **2011**, *137*, 985.
[46] T. Sinnberg, H. Niessner, M. P. Levesque, C. Dettweiler, C. Garbe, C. Busch, *Biol. Open* **2018**, *7*, bio032656.
[47] C. Busch, U. Drews, C. Garbe, S. R. Eisele, M. Oppitz, *Int. J. Oncol.* **2007**, *31*, 1367.
[48] P. Sharma, D. Patel, J. Chaudhary, *Cancer Med.* **2012**, *1*, 187.
[49] N. Cruz-Rodriguez, A. L. Combita, L. J. Enciso, L. F. Raney, P. L. Pinzon, O. C. Lozano, A. M. Campos, N. Peñaloza, J. Solano, M. V. Herrera, J. Zabaleta, S. Quijano, *J. Exp. Clin. Cancer Res.* **2017**, *36*, 37.
[50] J. Li, Y. Li, B. Wang, Y. Ma, P. Chen, *J. Biomed. Sci.* **2017**, *24*, 95.
[51] M. Schindl, S. F. Schoppmann, T. Ströbel, H. Heinzl, C. Leisser, R. Horvat, P. Birner, *Clin. Cancer Res.* **2003**, *9*, 779.
[52] H.-F. Yuen, Y.-P. Chan, K.-K. Chan, Y.-Y. Chu, M. L.-Y. Wong, S. Y.-K. Law, G. Srivastava, Y.-C. Wong, X. Wang, K.-W. Chan, *Br. J. Cancer* **2007**, *97*, 1409.
[53] S. F. Schoppmann, M. Schindl, G. Bayer, K. Aumayr, J. Dienes, R. Horvat, M. Rudas, M. Gnant, R. Jakesz, P. Birner, *Int. J. Cancer* **2003**, *104*, 677.
[54] Sachindra, L. L., D. Novak, H. Wu, L. Hüser, K. Granados, E. Orouji, J. Utikal, *Oncotarget* **2017**, *8*, 110166.
[55] C. Bohrer, S. Pfurr, K. Mammadzada, S. Schildge, L. Plappert, M. Hils, L. Pous, K. S. Rauch, V. I. Dumit, D. Pfeifer, J. Dengjel, M. Kirsch, K. Schachtrup, C. Schachtrup, *EMBO J.* **2015**, *34*, 2804.
[56] N. Zhang, R. K. Yantiss, H.-S. Nam, Y. Chin, X. K. Zhou, E. J. Scherl, B. P. Bosworth, K. Subbaramaiah, A. J. Dannenberg, R. Benezra, *Stem Cell Rep.* **2014**, *3*, 716.
[57] D. Lyden, A. Z. Young, D. Zagzag, W. Yan, W. Gerald, R. O'Reilly, B. L. Bader, R. O. Hynes, Y. Zhuang, K. Manova, R. Benezra, *Nature* **1999**, *401*, 670.
[58] Z. Dong, F. Wei, C. Zhou, T. Sumida, H. Hamakawa, Y. Hu, S. Liu, *Oral Oncol.* **2011**, *47*, 27.
[59] M. Papaspyridonos, I. Matei, Y. Huang, M. do Rosario Andre, H. Brazier-Mitouart, J. C. Waite, A. S. Chan, J. Kalter, I. Ramos, Q. Wu, C. Williams, J. D. Wolchok, P. B. Chapman, H. Peinado, N. Anandasabapathy, A. J. Ocean, R. N. Kaplan, J. P. Greenfield, J. Bromberg, D. Skokos, D. Lyden, *Nat. Commun.* **2015**, *6*, 6840.
[60] T. Maruyama, J. Li, J. P. Vaque, J. E. Konkel, W. Wang, B. Zhang, P. Zhang, B. F. Zamarron, D. Yu, Y. Wu, Y. Zhuang, J. S. Gutkind, W. Chen, *Nat. Immunol.* **2011**, *12*, 86.
[61] R. Ciarapica, J. Rosati, G. Cesareni, S. Nasi, *J. Biol. Chem.* **2003**, *278*, 12182.
[62] D. S. Mern, K. Hoppe-Seyler, F. Hoppe-Seyler, J. Hasskarl, B. Burwinkel, *Breast Cancer Res. Treat.* **2010**, *124*, 623.
[63] C. M. Tsang, K. C. P. Cheung, Y. C. Cheung, K. Man, V. W.-Y. Lui, S. W. Tsao, Y. Feng, *Biochim. Biophys. Acta* **2015**, *1852*, 541.
[64] K. Tada, K. Kawahara, S. Matsushita, T. Hashiguchi, I. Maruyama, T. Kanekura, *Phyther. Res.* **2012**, *26*, 833.
[65] P. Massi, A. Vaccani, S. Ceruti, A. Colombo, M. P. Abbracchio, D. Parolaro, *J. Pharmacol. Exp. Ther.* **2004**, *308*, 838.
[66] A. Ligresti, A. S. Moriello, K. Starowicz, I. Matias, S. Pisanti, L. De Petrocellis, C. Laezza, G. Portella, M. Bifulco, V. Di Marzo, *J. Pharmacol. Exp. Ther.* **2006**, *318*, 1375.
[67] S. D. McAllister, R. Murase, R. T. Christian, D. Lau, A. J. Zielinski, J. Allison, C. Almanza, A. Pakdel, J. Lee, C. Limbad, Y. Liu, R. J. Debs, D. H. Moore, P.-Y. Desprez, *Breast Cancer Res. Treat.* **2011**, *129*, 37.
[68] A. Shrivastava, P. M. Kuzontkoski, J. E. Groopman, A. Prasad, *Mol. Cancer Ther.* **2011**, *10*, 1161.
[69] H. M. Jensen, R. Korbut, P. W. Kania, K. Buchmann, *PLoS One* **2018**, *13*, 0200016.
[70] I. J. Fidler, *Nat. New Biol.* **1973**, *242*, 148.
[71] R. Lengagne, F.-A. Le Gal, M. Garcette, L. Fiette, P. Ave, M. Kato, J.-P. Briand, C. Massot, I. Nakashima, L. Rénia, J.-G. Guillet, A. Prévost-Blondel, *Cancer Res.* **2004**, *64*, 1496.
[72] F. R. Miller, B. E. Miller, G. H. Heppner, *Invasion Metastasis* **1983**, *3*, 22.
[73] V. Kuch, C. Schreiber, W. Thiele, V. Umansky, J. P. Sleeman, *Int. J. Cancer* **2013**, *132*, E94.
[74] J. M. Krachulec, G. Sedlmeier, W. Thiele, J. P. Sleeman, *Biochem. Cell Biol.* **2016**, *94*, 289.
[75] P. Mali, L. Yang, K. M. Esvelt, J. Aach, M. Guell, J. E. DiCarlo, J. E. Norville, G. M. Church, *Science* **2013**, *339*, 823.

[76] J. Schindelin, I. Arganda-Carreras, E. Frise, V. Kaynig, M. Longair, T. Pietzsch, S. Preibisch, C. Rueden, S. Saalfeld, B. Schmid, J.-Y. Tinevez, D. J. White, V. Hartenstein, K. Eliceiri, P. Tomancak, A. Cardona, *Nat. Methods* **2012**, *9*, 676.
[77] T. Lakshmikanth, S. Burke, T. H. Ali, S. Kimpfler, F. Ursini, L. Ruggeri, M. Capanni, V. Umansky, A. Paschen, A. Sucker, D. Pende, V. Groh, R. Biassoni, P. Höglund, M. Kato, K. Shibuya, D. Schadendorf, A. Anichini, S. Ferrone, A. Velardi, K. Kärre, A. Shibuya, E. Carbone, F. Colucci, *J. Clin. Invest.* **2009**, *119*, 1251.
[78] P. Muller, P. Schwille, T. Weidemann, *Bioinformatics* **2014**, *30*, 2532.
[79] C. T. Culbertson, S. C. Jacobson, J. Michael Ramsey, *Talanta* **2002**, *56*, 365.
[80] E. Cerami, J. Gao, U. Dogrusoz, B. E. Gross, S. O. Sumer, B. A. Aksoy, A. Jacobsen, C. J. Byrne, M. L. Heuer, E. Larsson, Y. Antipin, B. Reva, A. P. Goldberg, C. Sander, N. Schultz, *Cancer Discovery* **2012**, *2*, 401.
[81] J. Gao, B. A. Aksoy, U. Dogrusoz, G. Dresdner, B. Gross, S. O. Sumer, Y. Sun, A. Jacobsen, R. Sinha, E. Larsson, E. Cerami, C. Sander, N. Schultz, *Sci. Signaling* **2013**, *6*, pl1.
[82] D. P. Papahatjis, V. R. Nahmias, S. P. Nikas, T. Andreou, S. O. Alapafuja, A. Tsotinis, J. Guo, P. Fan, A. Makriyannis, *J. Med. Chem.* **2007**, *50*, 4048.
[83] N. Volz, *Sauerstoff-Heterocyclen Als Neue, Selektive Liganden Für Die Cannabinoid-Rezeptoren*, Logos-Verl, USA **2010**.
[84] Y. Hu, G. K. Smyth, *J. Immunol. Methods* **2009**, *347*, 70.